AN EXPERIMENTAL AND ANALYTICAL STUDY OF THE WEAR OF PAPER MACHINE FORMING FABRICS

Richard Charles Batty

A Dissertation

in

The Faculty

of

Engineering

Presented in Partial Fulfillment of the Requirements
for the degree of Master of Engineering at
Concordia University
Montréal, Québec, Canada

August 1979

© Richard Charles Batty, 1979

ABSTRACT

AN EXPERIMENTAL AND ANALYTICAL STUDY OF THE WEAR OF PAPER MACHINE FORMING FABRICS

Richard Charles Batty, M.Eng.
Concordia University, 1979

The origin and causes of the wear of paper machine forming fabrics are described. Experimental results from tests during which various types of forming fabrics were worn on a test machine are presented. They indicate that a fabric's resistance to wear is proportional to the amount of material available for wear before the fabric is worn out. A mathematical model is proposed which, given the design parameters of a forming fabric, would predict the rate of wear of the fabric compared to that of a fabric which had already been worn out. The bottom shute knuckle of the forming fabric is modelled as a section of a torus, or hoop, and a relationship is derived for its volume as a function of the distance from its outside edge. This volume is related to the time on the test machine required to produce varying amounts of wear on the fabric and thus the experimental and theoretical results may be compared. The model is seen to predict quite accurately the relative wear resistance of various forming fabric designs.

ACKNOWLEDGEMENTS

The author would like to thank J.W.I. Ltd. for their permission to publish the experimental results included in this paper, Mr. Dennis Allenger for his assistance with the mathematical derivation, and Prof. S. Katz, his supervisor, for his encouragement and assistance in the preparation of this dissertation.

TABLE OF CONTENTS

LIST OF FIGURES AND TABLES

FIGURES

TABLES

LIST OF SYMBOLS

d = shute strand diameter

g = length of perpendicular from center of torus cross-section to PQ

h = length of the perpendicular from P to x-axis

m = length of chord PQ

r = shute strand radius

t = distance along x-axis from x = R toward origin which represents the loss of strand thickness due to wear

t_0 = distance from x = R to base of perpendicular of length h

t_1 = distance from T to base of perpendicular of length h

x = coordinate in whose direction fabric wear occurs

y = third member of a 3-dimensional cartesian coordinate system

z = central coordinate through torus

C = thickness of fabric

O = origin of coordinate system

P = intersection of perpendicular from S to outer edge of torus

P' = arbitrary point on the perpendicular from P to x-axis

Q = point of intersection with PO with inner edge of torus

Q' = point of intersection with P'O with inner edge of torus

R = outer radius of torus

S = end point of the distance t along the x-axis

T = centre of the torus cross-section

V = volume of a section of the torus

V_p = volume of the torus section, valid to $t = t_o$

V_Q = volume of the torus section, valid to $t_0 \leq t \leq (R-d)$

dV = infinitesimal volume used to set up volume integral

W = loss of strand thickness when 100% wear is reached

$\alpha = r/(R-r)$

$\beta = (R-t)/(R-r)$

$\gamma = \cos\lambda_{min}$

$\delta = \sin\lambda_{min}$

θ = angle between the xy plane and projection on the xy plane of radius to dV

λ = angle between P'O and the x-axis

λ_{min} = angle between PQ and the x-axis

λ_{max} = λ when PO is tangent to the torus

ρ = radius to dV in spherical coordinates

ϕ = angle between the z-axis and radius to dV, also between PO and the z-axis

ϕ_{min} = ϕ when PO is tangent to the torus

CHAPTER 1

INTRODUCTION AND BACKGROUND

1.1. The Development of Papermaking

In the year 105 A.D., an official at the imperial court of China by the name of Ts'ai Lun invented what has become one of the most versatile and widely used materials the world over - paper. Paper was originally used for recording information but while this remains a very important use, many other applications have arisen over the years. These include the disseminating of information in the form of books, leaflets, posters, newspapers, drawings and letters and also widely varying uses such as wrapping, packaging, containers, towelling, photography, labelling, currency, postage stamps and so forth. Types of paper have become equally as numerous as the functions they serve.

Ts'ai Lun made paper not out of wood or synthetic fibres, but out of fibres from rags, fish nets or ropes beaten in water to form a slurry. He dipped a screen into a container of this slurry and upon removal of the screen, drainage of water left a wet mat of fibres. The mat, or sheet of paper, was left to dry to allow evaporation of the remaining water. This method of making one sheet at a time was the process which travelled from China to Japan, the Arab Countries, Europe and eventually to North America. The process remained basically unchanged until the eighteenth century when the Industrial Revolution improved the

efficiency of the papermaking process with the invention of the paper machine. In 1798, the French government granted a patent to Nicolas-Louis Robert, who built a moving screen to receive a continuous supply of slurry so as to form a continuous sheet of paper. But the paper machine did not become an industrial entity until a patent was granted in 1807 for an improved version of Robert's machine. This machine was devised by two English engineers who worked for the firm of Henry and Sealy Fourdrinier. It is by the name of Fourdrinier that the most common type of paper machine is still known. In 1809 John Dickinson, an English papermaker, invented another type of paper machine, the cylinder machine. Despite undergoing many technological developments, these two types of papermachine are in principle unchanged. Several new types of paper machine have been invented during the past few years, but they also make use of the idea of draining water through a screen which conveys the slurry of paper fibres.

1.2. Description of the Paper Forming Process

Wood is the chief source of paper fibres. Individual fibres are obtained by disintegrating (pulping) the wood either mechanically and/or chemically and after several processes including screening, cleaning, bleaching, mixing, blending, refining and the addition of additives, the resulting pulp is diluted from about three percent consistency to approximately 0.5 to 0.7 percent. This extremely low

ratio of fibre to water is required to enable even distribution of the fibres as they are dispersed by a headbox onto the moving screen which is commonly referred to as the wire. As previously mentioned, the function of the wire is to drain as much water as possible from the pulp and form a sheet of paper which can then be satisfactorily transferred to the next part of the paper machine, the press section, where more water is removed by mechanical pressing action. Paper quality standards are high and thus the fourdrinier (wire section) must be carefully designed and operated to optimize the paper formation process. The wire itself is of critical importance in the process since it must permit the dispersed individual fibres in the dilute pulp stock to be retained evenly across the machine while allowing as much water as possible to drain from the stock. Undue variations in thickness and dispersal of fibres are totally unacceptable whether in local areas or right across the width of the paper machine. Furthermore, the sheet of paper must usually be smooth and thus the wire must not impress a serious pattern, known as wire mark, on the paper. The wire must be designed such that the sheet of paper can be removed from it without difficulty for transfer to the press section. These requirements place stringent demands on the wire and thus over the years, the design of the wires to maximize wear properties had of necessity to take second place to the design for good paper properties.

1.3. Causes of Wear in Papermachine Forming Wires

Rapid wear of fourdrinier wires resulted as paper machines were increased in speed and as various developments were implemented to enhance drainage. Wear was in fact inevitable due to the nature of the fourdrinier machine since wear will occur whenever two surfaces are in contact. If the two surfaces are moving one with respect to the other, the situation is worsened and generally more wear will occur the greater the speed differential. Various other factors such as an increase in the normal force between the materials that make up the two surfaces can accelerate a wear problem.

Wear involves the unwanted removal of material from a surface and may be caused by any one or combination of four mechanisms. These are adhesive or galling wear, abrasive or cutting wear, corrosion wear and surface fatigue. The action of these different mechanisms as they relate to the Fourdrinier paper machine has been well described by Pye (1). While all four may occur on a paper machine, the most serious as far as the fourdrinier wire is concerned is abrasive wear. As depicted in Figure 1, the wire is an endless belt which travels through a path around several rolls and over certain stationary surfaces. Theoretically, adhesive wear only should occur on the wire due to the contact with the rolls. However, a speed differential may occur between a roll and the wire if, for example, a bearing begins to seize. In this case the wear will be abrasive

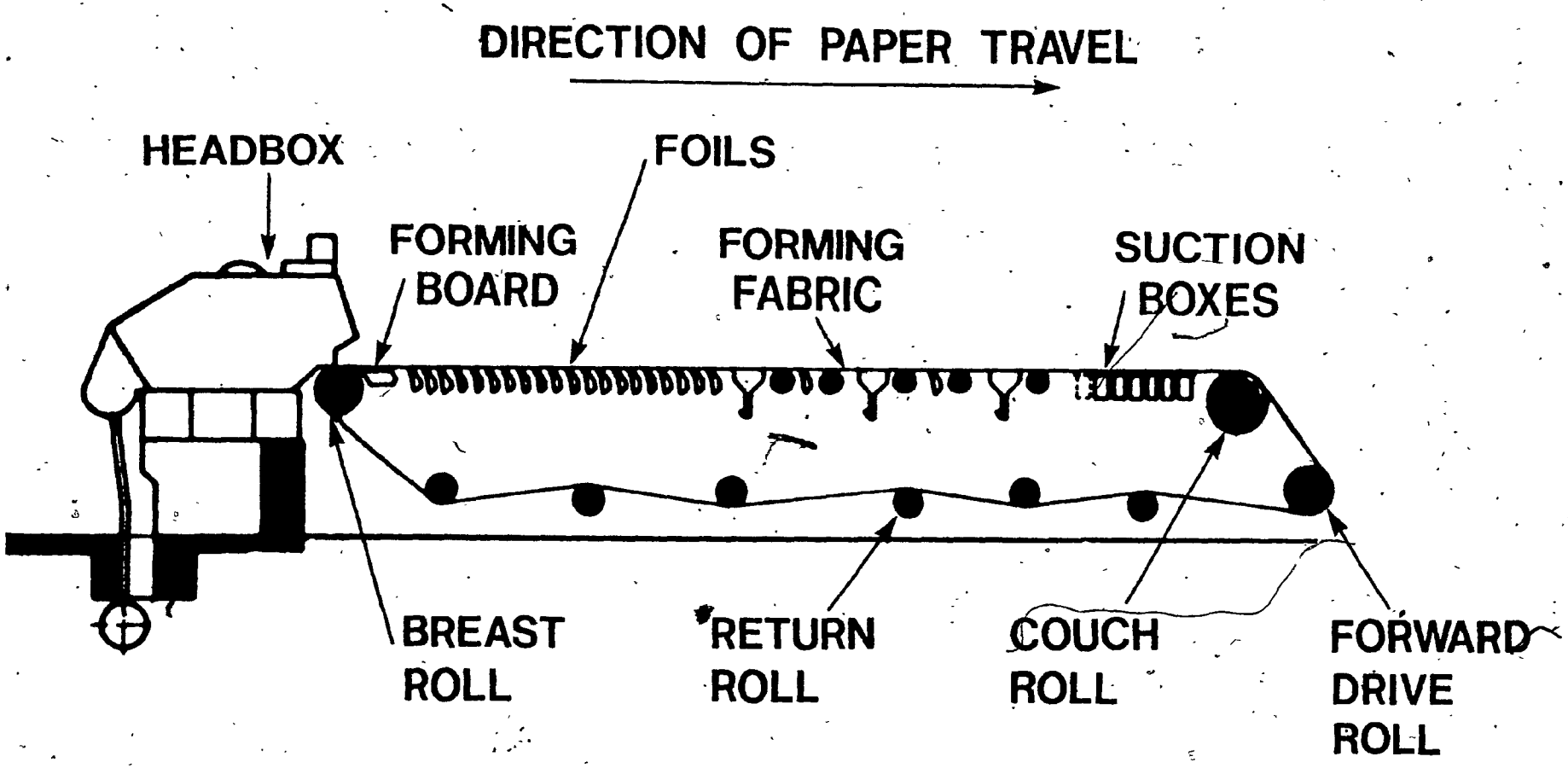

Figure 1. Fourdrinier Papermachine

and the rate of wear will be much greater than if adhesive wear only was taking place. The abrasive action will be more severe and the rate of wear greatly accelerated if not only is there relative motion between wire and roll, but also the surface of the roll deteriorates as is sometimes the case.

Stationary drainage elements on the fourdrinier machine include forming boards, foil blades and suction boxes. Forming boards and foil blades, which replaced table rolls, are generally made from high molecular weight polyethylene or ceramics such as aluminum oxides. Foil blades may have inserts made from aluminum oxide, silicon, tungsten or titanium carbides or similar very hard materials to protect the polyethylene. These materials pose no abrasion problem when their surface is smooth, but if the leading protrudes or segments become chipped or separated exposing a sharp corner, their action on a wire is almost as severe as that of a knife. Suction box covers are also made from polyethylene, ceramics or the carbides mentioned above. While less prone to separation of segments or chipping, they may inflict considerable abrasive, or drag, wear on a wire since the high suction forces deflect the wire into the sharp-edged holes of the cover (2). Suction box covers have been shown to be the major cause of wear on a fourdrinier wire (3).

Speed differentials between the wire and a roll may occur due to factors other than the seized bearing mentioned

above (4). Slippage of the wire on a roll (most often the couch roll) may result from a high tension differential in the wire from one side of the roll to the other, causing what is known as creep wear (5). The severity of the abrasive action will depend on the condition of the roll surface and on whether the wire is deflected into suction holes. A roll which deflects such that its central axis does not coincide with its axis of rotation will cause part of the wire to travel faster than the roll and another part of the wire to travel slower than the roll (4). Thus both drag and creep wear will occur on the wire.

It is inevitable that some grit, especially from the groundwood mill pulp stones (6), passes through the stock cleaning system and while the finer particles may pass through the wire during the drainage process, the larger particles may become entrapped in the wire mesh and cause gouging damage to stationary elements and roll surfaces (3, 4). Once this happens, the damaged surface may in turn cause wear of the wire. Grit may also become imbedded in the various stationary surfaces, similarly damaging the wire. The same problems may also arise due to the use of fillers such as kaolin (china clay) which contain abrasive impurities (7).

Until about twenty years ago, forming wires were generally made of phosphor bronze and were usually worn out within ten days. It was felt that metal strands were required to resist the tensile forces (approx. 40 pounds per

inch of width) to which wires were subjected. However, the development of polyester filaments and the use of different weave patterns yielded sufficiently high elastic moduli for papermaking application (8) and gave birth to a new era: by 1975, seventy percent of all fourdrinier paper machines in the United States had switched from metal wires to plastic forming fabrics (9). Average life of these fabrics was 4.5 times that of bronze wires. This was a vast improvement. However, the potential for even further improvement existed and efforts to reduce clothing costs and to reduce machine downtime by improving fabric life have continued.

1.4. Aim of this Study

As has been explained, there are thus many causes of abrasive wear of forming fabrics. The obvious approach to insure good fabric life is to eliminate these causes or certainly to minimize them as much as possible. However, the best possible technology is employed to avoid these problems within financial constraints. In other words, vast expenditures would be required to purchase rolls with practically zero deflection or to provide screening processes which would all but eliminate grit from the stock. Given that the paper companies must of necessity sacrifice fabric life for economic reasons, the inevitable question is how can fabric life be maximized within these constraints? This is one of the roles of the paper machine clothing manufacturer. With this in mind, J.W.I. Ltd. decided to investigate how its major

product, paper machine forming fabrics, could be optimized from a design viewpoint while maintaining good papermaking properties.

Forming fabrics are woven on looms, either as a continuous belt or as a flat piece, the two ends being subsequently joined together in a seam. The most commonly used weave patterns are the four-shed and five-shed patterns (4,8). In the former, strands in the cross machine direction (shute strands) pass over one machine direction strand (warp strand) and under the next three machine direction strands. In the latter, the shute strand passes over one warp strand and under the next four warp strands (see figure 2). These are the two weave patterns that are dealt with in this paper.

Different types of paper are made on different designs of forming fabric. Apart from weave pattern, the fabric design parameters which may vary are mesh, strand size and strand material. This paper attempts to shed light on how the amount of strand material available for wear is dependent on these parameters for a given type of strand material.

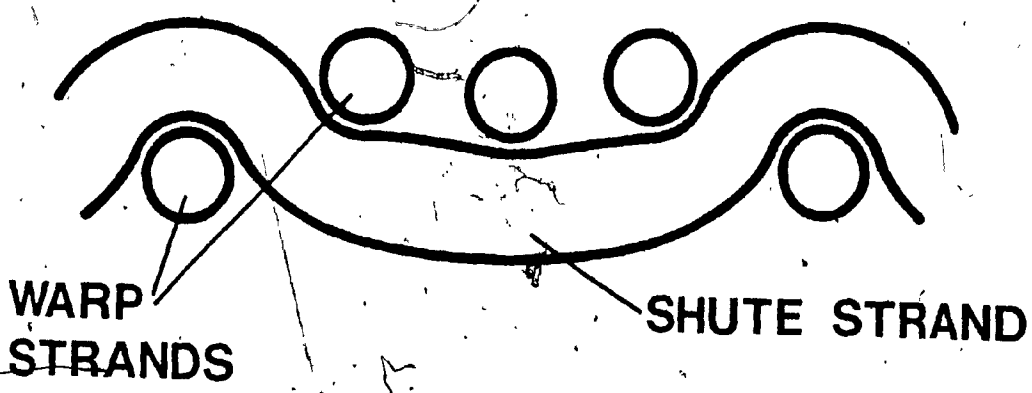

4-SHED WEAVE PATTERN

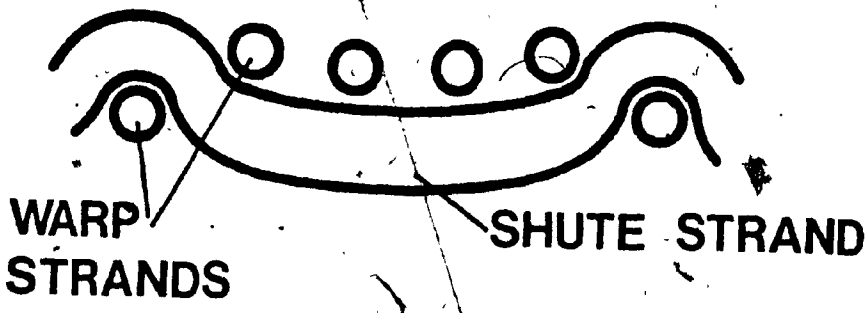

5-SHED WEAVE PATTERN

Figure 2. The Most Common Forming Fabric Weave Patterns.

Machine direction is into the plane of the paper.

CHAPTER 2

THE MATHEMATICAL MODEL

2.1. Explanation of the Mathematical Model

Fabrics are held together by the process of weaving which entails interlocking of the warp and shute strands. Both types of strands thus pass from the top to the bottom of the fabric according to the weave pattern. The process of heat setting after manufacturing applies heat to the fabric as it is held under tension and stretches it to the required dimensions while ensuring that the fabric will be stable and will not stretch during operation. Heat setting determines the final geometry of the fabric including the amount of curvature in the strands.

After heat setting the warp strands are relatively straight and the shute strands quite curved due to the tension and heat that have been applied. The sections of a strand as it passes over or under a strand perpendicular to it are known as knuckles. This term is most usually applied to the shute strands because of their more pronounced curvature. In the four and five-shed forming fabric designs, the most common for papermaking, the bottom shute knuckles form the bottom surface of the fabric as it passes over rolls, foils and suction boxes. They thus suffer most of the wear during the fabric's life. (In most cases, 100% wear is reached before wear begins to occur on the warp strands. (See Figure 3). The reason for this geometry stems from the desire of the fabric manufacturers to avoid wear on the warp strands

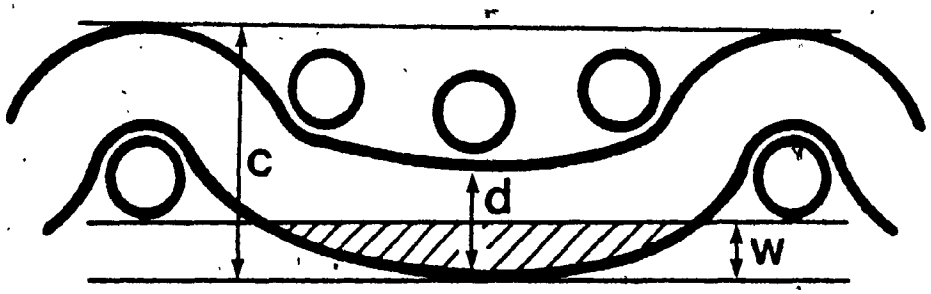

c = FABRIC CALIPER
d = SHUTE STRAND DIAMETER
w = 100% WEAR LINE
BY DEFINITION w = 0.58d

Figure 3. The Definition of Fabric Percent Wear

Machine direction strands are again into the plane of the paper

N.B. Warp strands are still above the wearing surface at 100% wear. Shaded section indicates material removed at 100% wear.

since this could lead to a loss in elastic modulus resulting in stretching of the fabric.

A fabric is considered to be 100% worn when 58% of the diameter of the shute knuckle has been worn away (Figure 3). This criterion has been continued from the old practice of considering metal wires 100% worn when 58% of the warp diameter was worn. This definition was the result of work by Prof. Keay at Consolidated Paper Corporation who found that this figure represented the average wear on a wire when it was removed from the paper machine (10).

During my work, comparative testing for abrasion resistance of various fabrics at J.W.I. Ltd., percent wear was plotted against the number of cycles. I observed that the rate of wear decreased during the life of a fabric. This seemed to indicate that as the bottom knuckles wore and the wearing surface of the knuckles became larger, resistance to the abrasive action increased. It implied that the amount of material removed from the knuckle during each pass of the test machine reciprocating component used to produce wear (description given later) was approximately the same. Since this volume was nearly the same and the area was constantly increasing, obviously the depth of the material removed per cycle became less and less.

To explain this phenomenon, I developed a mathematical model. The bottom shute knuckle of a fabric very closely resembles a section of a torus or hoop. Its geometry is defined by a radius of curvature determined by both warp and

shute diameters and mesh after heat setting and by the diameter of the strand which forms the knuckle. By obtaining the volume of the torus as a function of distance from the outer surface (Figure 4), a comparison could be made between the theoretical curves obtained and those resulting from the experiments. If applicable, such a model would be extremely useful in predicting how well a particular fabric would resist abrasion.

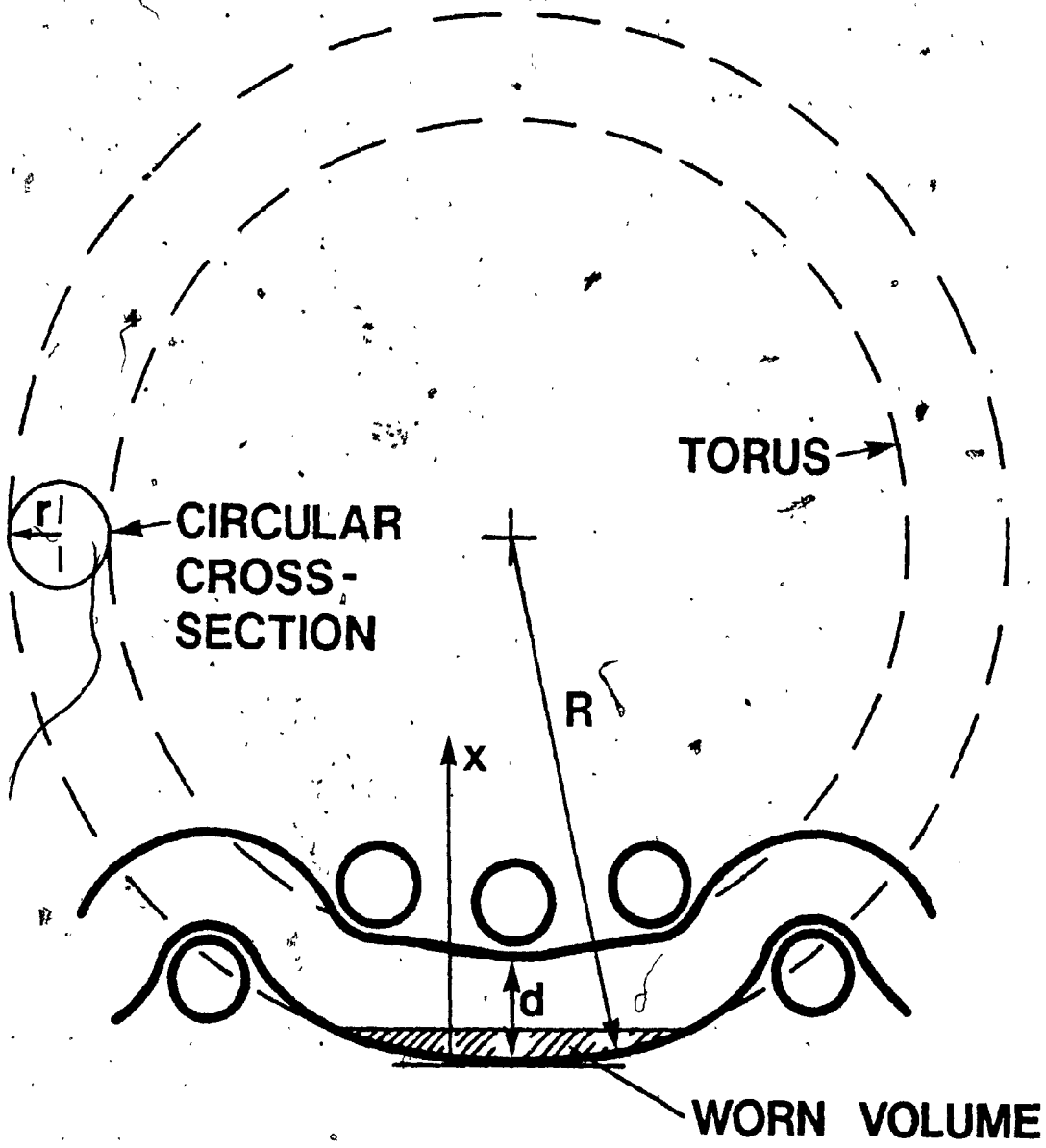

Figure 4. Modelling the Shute Strand as a Section of a Torus

The model obtains the worn volume (shaded area) as a function of the coordinate x

2.2. Derivation of the Volume Integral

Consider the torus section shown in Figure 5.

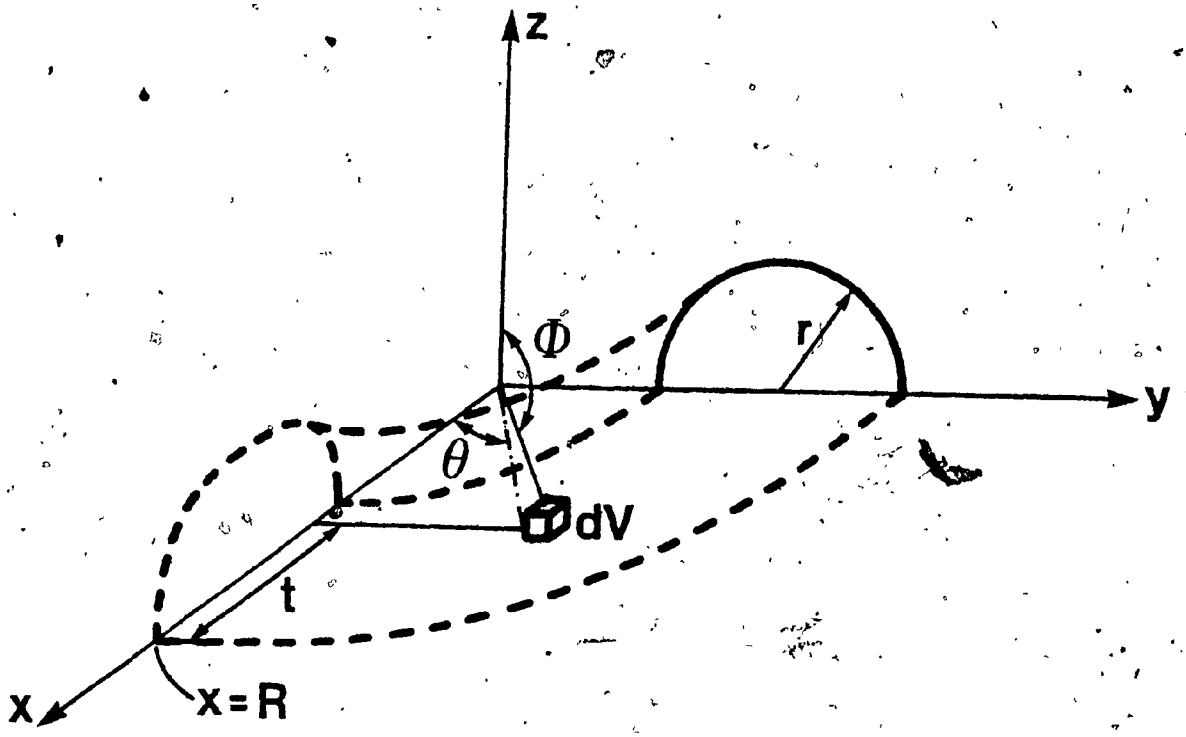

Figure 5. Section of a Torus in Three Dimensions

Consider an infinitesimal volume dV. Let R be the outer radius of the torus, and r the radius of its circular cross-section. Let ϕ be an angle between the radius from the origin to dV and the z-axis. Let θ be the angle between the projection of this radius on the xy plane and the x-axis. Let t be the difference between the outer radius of the torus R and the x-coordinate of dV.

For the purpose of this paper it is necessary to find V, the volume of the torus as a function of t, which starts

from zero at x = R and gets larger moving along the x-axis toward the origin. (See Figure 6 - the volume V is indicated by the shaded section).

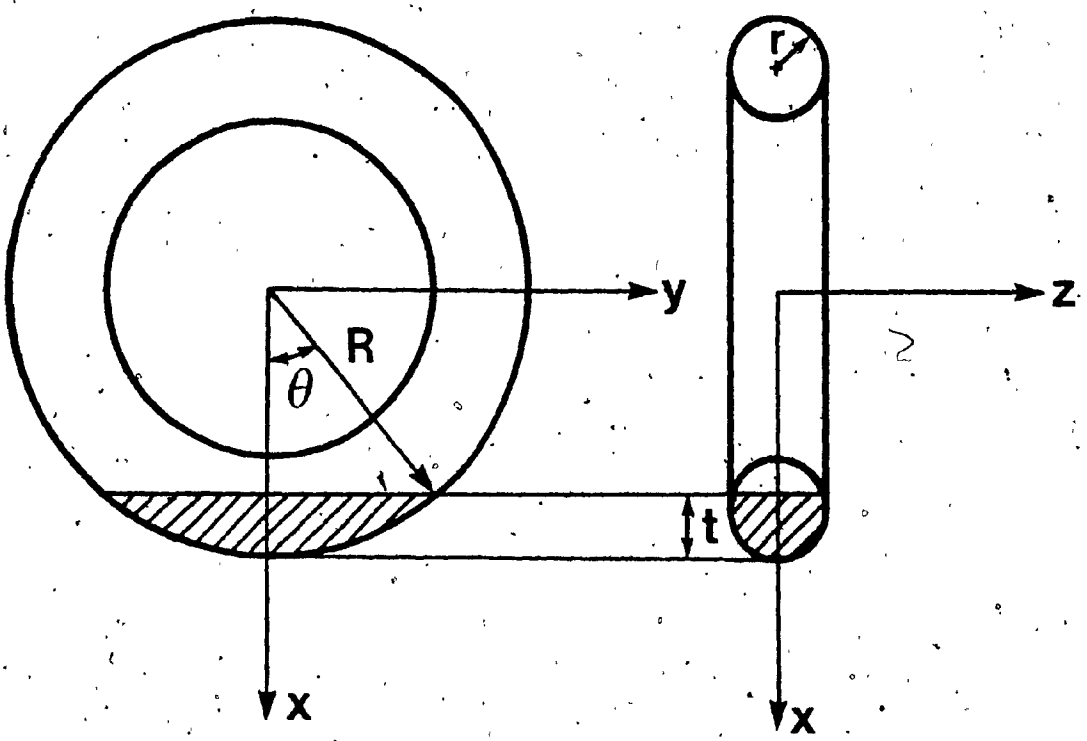

Figure 6. The Torus in Cross-section

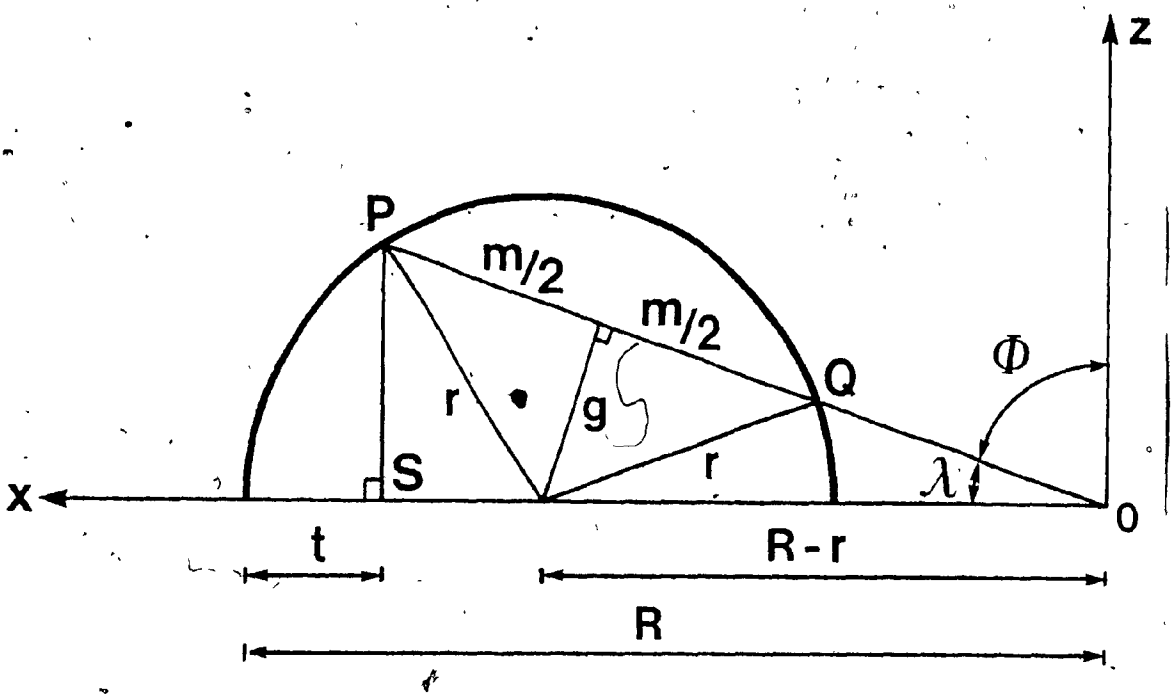

Figure 7. Section of the Torus showing the Integral Variables in the xz plane

Consider now Figure 7, which shows a view of the torus in the xz plane.

1. t is an arbitrary distance along the x-axis from x = R (the outer edge of the torus)
2. PS is the perpendicular drawn from t to intersect the torus
3. P is joined to the origin and intersects the inside surface of the torus at Q
4. The circular cross-section of the torus has radius r.
5. g is the perpendicular drawn from the centre of this circular cross-section to PQ
6. This center will by definition be (R-r) from the origin
7. ϕ is the angle between PO and the z-axis
8. λ is the angle between PO and the x-axis
9. m is the chord from P to Q

Expressions must be obtained for PO, QO and since these parameters will be variables in the volume integral. Now

$$\sin\lambda = \frac{g}{R-r} \qquad (1)$$

and since

$$r^2 = (g)^2 + \left(\frac{m}{2}\right)^2 \qquad (2)$$

By substituting equation (1) into equation (2) and performing some algebraic and trigonometric manipulation,

$$m = 2\sqrt{r^2\cos^2\lambda - R(R-2r)\sin^2\lambda} \qquad (3)$$

Let $|Q|$ be the distance from the origin to Q and $|P|$ the distance from the origin to P. Therefore

$$|Q| + \frac{m}{2} = (R-r)\cos\lambda \qquad (4)$$

By substituting equation (3) into equation (4)

$$|Q| = (R-r)\cos\lambda - \sqrt{r^2\cos^2\lambda - R(R-2r)\sin^2\lambda} \qquad (5)$$

Since $|P| = |Q| + m \qquad (6)$

By substituting equation (3) and equation (5) into equation (6) one obtains

$$|P| = (R-r)\cos\lambda + \sqrt{r^2\cos^2\lambda - R(R-2r)\sin^2\lambda} \qquad (7)$$

Consider Figure 8 which again shows a cross-section of the torus in the xz plane:

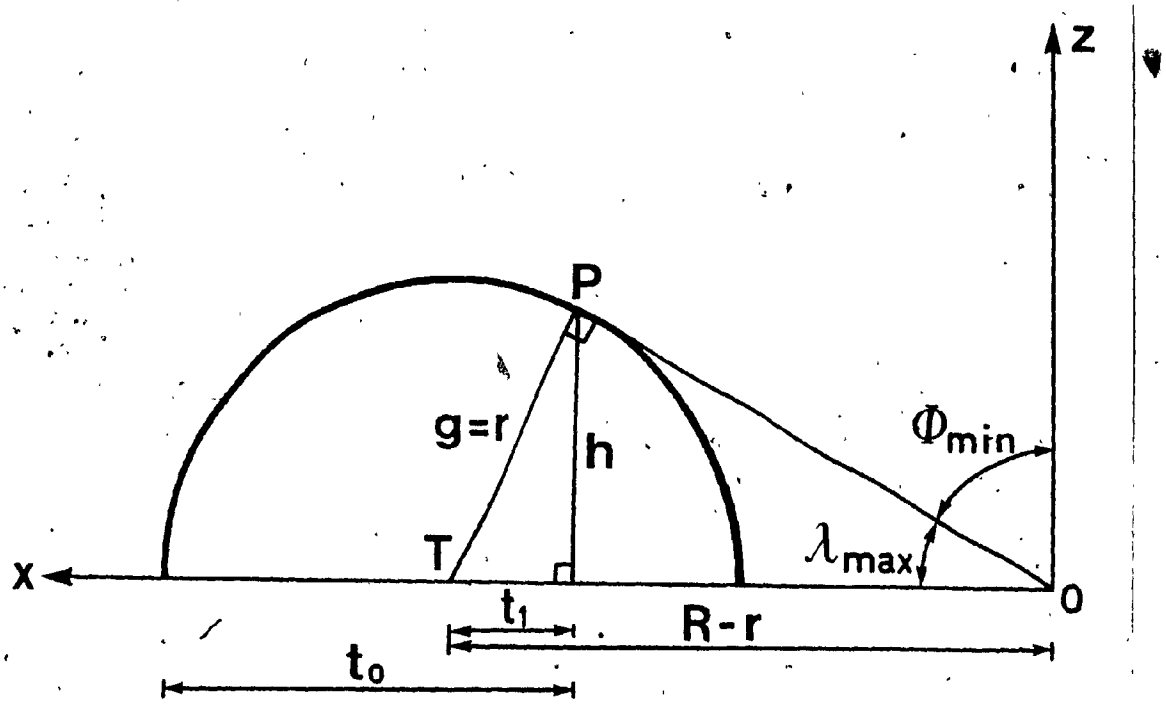

Figure 8. Cross-section of the Torus in the xz Plane showing the Critical Dimension t_1

When PO is tangent to the circle, let t have a value of t_o. If $t<t_o$, only one integral (V_P) is required to give the volume V; however, if $t>t_o$, two separate integrals must be added together, (V_P+V_Q), since the limits of integration are different in this case. When PO is tangent to the circle, λ will be at its maximum, ϕ at its minimum, g will be equal to r and |P| equal to |OT|. To obtain ϕ_{min}, it is known that

$$\sin(\lambda_{max}) = \frac{r}{R-r} \qquad (8)$$

Rearranging, one obtains

$$\lambda_{max} = \sin^{-1} \frac{r}{R-r} \qquad (9)$$

Now $$\phi_{min} = \left(\frac{\pi}{2} - \lambda_{max}\right) \qquad (10)$$

Therefore

$$\phi_{min} = \cos^{-1} \frac{r}{R-r} \qquad (11)$$

and $$\phi_{min} = \sin^{-1} \frac{R}{R-r}\sqrt{1-\frac{2r}{R}} \qquad (12)$$

Referring again to Figure 8, h is the perpendicular from P to the x-axis. To determine t_o as a function of R and r let t_1 be the distance from the torus cross-section centre to the base of the perpendicular h. Therefore

$$t_1 = t_o - r \qquad (13)$$

Now $$t_1^2 = r^2 - h^2 \qquad (14)$$

and also

$$h^2 = |Q|^2 - (R-t_o)^2 \qquad (15)$$

By substituting equation (15) into equation (14) and re-arranging one obtains

$$r^2 - |Q|^2 = t_1^2 - (R-t_o)^2 \qquad (16)$$

It is known that

$$r^2 + |Q|^2 = (t_1 + R - t_o)^2 \qquad (17)$$

If one manipulates equation (16) and equation (17), substitutes equation (13) and solves for t_o, one obtains

$$t_o = Rr/(R-r) \qquad (18)$$

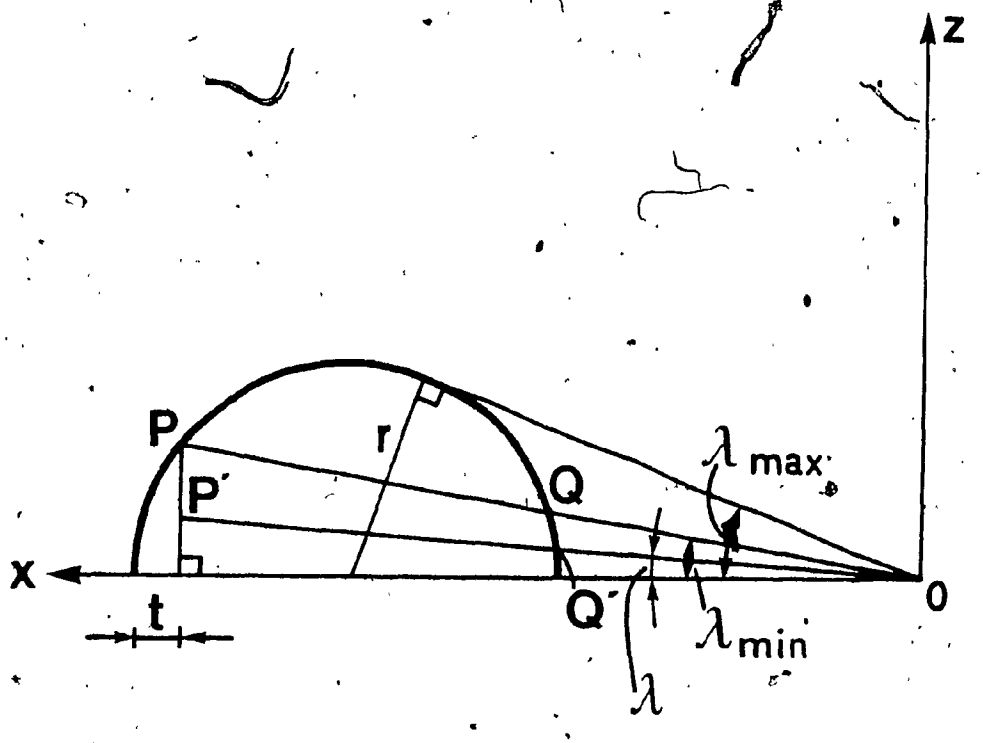

Figure 9. Cross-section of the Torus in the xz Plane showing several of the limits of integration

Referring to Figure 9, P' is any arbitrary point on the perpendicular from P to the x-axis. Q' is the point at which P'O intersects the inner side of the torus. λ_{min} is the angle formed by PO and the x-axis and λ_{max} is the angle between the tangent from the origin to the torus and the x-axis.

It is required to determine the length of $|P'|$, since this dimension will be a limit in the integral.

It is also known that for any λ

$$|Q'| = (R-r)\cos\lambda - \sqrt{r^2-(R-r)^2\sin^2\lambda} \qquad (19)$$

Letting $\frac{r}{R-r} = \alpha$, one obtains (20)

$$|Q'| = (R-r)\{\cos\lambda - \sqrt{\alpha^2-\sin^2\lambda}\} \qquad (21)$$

and $$|P'| = \frac{R-t}{\cos\lambda} \qquad (22)$$

It is now possible to compute λ_{min}, another of the limits of the integral.

$$\cos\lambda_{min} = \frac{R-t}{|P'|_{max}} \qquad (23)$$

Substituting for $|P'|_{max}$, one obtains

$$\cos\lambda_{min} = \frac{R-t}{(R-r)\{\cos\lambda_{min} + \sqrt{\alpha^2-\sin^2\lambda_{min}}\}} \qquad (24)$$

Letting $\frac{R-t}{R-r} = \beta$, and rearranging, (25)

$$\cos^2\lambda_{min} + \cos\lambda_{min}\sqrt{\alpha^2-\sin^2\lambda_{min}} = \beta \qquad (26)$$

Expanding equation (26), rearranging and solving for $\cos\lambda_{min}$

$$\cos\lambda_{min} = \frac{\beta}{\sqrt{\alpha^2-1+2\beta}} \qquad (27)$$

Solving for $\sin\lambda_{min}$, one obtains

$$\sin\lambda_{min} = \sqrt{1 - \frac{\beta^2}{\alpha^2-1+2\beta}} \qquad (28)$$

The lengths of the vectors $|P|$ and $|Q|$ have already been computed. Substituting equation (20) and equation (25)

$$|Q| = (R-r)(\cos\lambda - \sqrt{a^2-\sin^2\lambda}) \tag{32}$$

$$|P| = (R-r)(\cos\lambda + \sqrt{a^2-\sin^2\lambda}) \tag{33}$$

Also $$\sin\lambda_{max} = a \tag{34}$$

$$\cos\lambda_{max} = \sqrt{1-a^2} \tag{35}$$

All the relationships required for computing the integral have now been obtained.

In spherical coordinates, an infinitesimal volume dV is given by,

$$dV = \rho^2 \sin\phi d\rho d\phi d\theta \tag{36}$$

In this particular case, for $t \leq t_o$, the volume integral with the appropriate limits will be

$$V_p = 4\int_o^{\theta}\int_{\frac{\pi}{2}-\lambda_{min}}^{\frac{\pi}{2}}\int_{|P'|}^{R} \rho^2 \sin\phi d\rho d\phi d\theta \tag{37}$$

$$= \frac{4}{3}\int_o^{\theta}\int_{\frac{\pi}{2}-\lambda_{min}}^{\frac{\pi}{2}} \sin\phi\{R^3 - (\frac{R-t}{\sin\phi})^3\} d\phi d\theta \tag{38}$$

$$= -\frac{4}{3}R^3\int_o^{\theta}\cos\phi\Big|_{\frac{\pi}{2}-\lambda_{min}}^{\frac{\pi}{2}} d\theta - \frac{4}{3}(R-t)^3\int_o^{\theta}\int_{\frac{\pi}{2}-\lambda_{min}}^{\frac{\pi}{2}} \frac{d\phi d\theta}{\sin^2\phi} \tag{39}$$

Letting $\cos\lambda_{min} = \gamma$ and $\sin\lambda_{min} = \delta$, one obtains (40,41)

Therefore

$$V_p = -\frac{4}{3}R^3\int_o^{\theta}(0-\delta)d\theta - \frac{4}{3}(R-t)^3\int_o^{\theta}\frac{\delta}{\gamma}\,d\theta \tag{42}$$

$$= \frac{4}{3}R^3\delta\theta - \frac{4}{3}\beta^3(R-r)^3\frac{\delta}{\gamma}\,\theta \tag{43}$$

Therefore, for the first part of the integral,

$$V_P = \frac{4}{3}\delta\theta\,(R^3 - \frac{\beta^3(R-r)^3}{\gamma}) \tag{44}$$

When $t>t_o$, another integral is used since the limits are now different. Let this integral be V_Q.

As before

$$dV = \rho^2\sin\phi\,d\phi\,d\theta\,d\rho \tag{45}$$

The volume integral with the appropriate limits is

$$V_Q = 4\int_0^{\theta}\int_{\frac{\pi}{2}-\lambda_{max}}^{\frac{\pi}{2}-\lambda_{min}}\int_{|P'|}^{(R-t_o)\tan\lambda} \rho^2\sin\phi\,d\rho\,d\phi\,d\theta \tag{46}$$

$$= \frac{4}{3}\int_0^{\theta}\int_{\frac{\pi}{2}-\lambda_{max}}^{\frac{\pi}{2}-\lambda_{min}} \sin\phi\{(R-t_o)^3\cot^3\phi-(\frac{R-t}{\sin\phi})^3\}d\phi\,d\theta \tag{47}$$

$$= \frac{4}{3}\int_0^{\theta}\int_{\frac{\pi}{2}-\lambda_{max}}^{\frac{\pi}{2}-\lambda_{min}} (R-t_o)^3\sin\phi\cot^3\phi\,d\phi\,d\theta - \frac{4}{3}(R-t)^3\int_0^{\theta}\int_{\frac{\pi}{2}-\lambda_{max}}^{\frac{\pi}{2}-\lambda_{min}} \frac{d\phi\,d\theta}{\sin^2\phi} \tag{48}$$

$$= \frac{4}{3}\int_0^{\theta}(R-t_o)^3(\frac{1}{32}\cos4\phi-\frac{1}{4}\cos^2\phi\cos2\phi)\Big|_{\frac{\pi}{2}-\lambda_{max}}^{\frac{\pi}{2}-\lambda_{min}} d\theta-\frac{4}{3}(R-t)^3\int_0^{\theta}(-\cot\phi)\Big|_{\frac{\pi}{2}-\lambda_{max}}^{\frac{\pi}{2}-\lambda_{min}} d\theta \tag{49}$$

$$= \frac{4}{3}(R-t_o)^3\int_0^{\theta}\{\frac{1}{32}(4\cos^4\phi-8\cos^2\phi+1)-\frac{1}{4}\cos^2\phi(2\cos^2\phi-1)\}\Big|_{\frac{\pi}{2}-\lambda_{max}}^{\frac{\pi}{2}-\lambda_{min}} d\theta$$

$$- \frac{4}{3}\beta^3(R-r)^3\int_0^{\theta}(-\cot\phi)\Big|_{\frac{\pi}{2}-\lambda_{max}}^{\frac{\pi}{2}-\lambda_{min}} d\theta \tag{50}$$

$$= \frac{4}{3}(R-t_o)^3 \int_o^\theta \left\{ \frac{1}{32}(4\delta^4-8\delta^2+1) - \frac{1}{4}\delta^2(2\delta^2-1) - \frac{1}{32}\{4(\frac{r}{R-r})^4 - 8(\frac{r}{R-r})^2+1\} \right.$$

$$\left. + \frac{1}{4}(\frac{r}{R-r})^2\{2(\frac{r}{R-r})^2-1\} \right\} d\theta + \frac{4}{3}\beta^3(R-r)^3 \int_o^\theta (\frac{\gamma}{\delta} - \sqrt{\frac{1-\alpha^2}{\alpha^2}}) \, d\theta \quad (51)$$

$$= \frac{4}{3}(R-t_o)^3\{\frac{\delta^4}{8} - \frac{\delta^2}{4} + \frac{1}{32} - \frac{\delta^4}{2} + \frac{\delta^2}{4} - \frac{\alpha^4}{8} - \frac{1}{32} + \frac{\alpha^4}{2} - \frac{\alpha^2}{4}\} \theta$$

$$+ \frac{4}{3}\beta^3(R-r)^3\{\frac{\gamma}{\delta} - \sqrt{\frac{1-\alpha^2}{\alpha^2}}\} \theta \quad (52)$$

Therefore the second part of the integral is

$$V_Q = \frac{4}{3}\theta(R-t_o)^3\{\frac{3\alpha^4}{8} - \frac{3\delta^4}{8}\} + \frac{4}{3}\theta\beta^3(R-r)^3\{\frac{\gamma}{\delta} - \sqrt{\frac{1-\alpha^2}{\alpha^2}}\} \quad (53)$$

Values for R and r are given (measured from a sample strand); α, β and t_o are functions of R, r and t; δ and γ are functions of α and β. V_P and V_Q may thus be determined as functions of θ and θ is a function of t:

$$\theta = \cos^{-1}\frac{R-t}{R} \quad \text{(See Figure 10)} \quad (54)$$

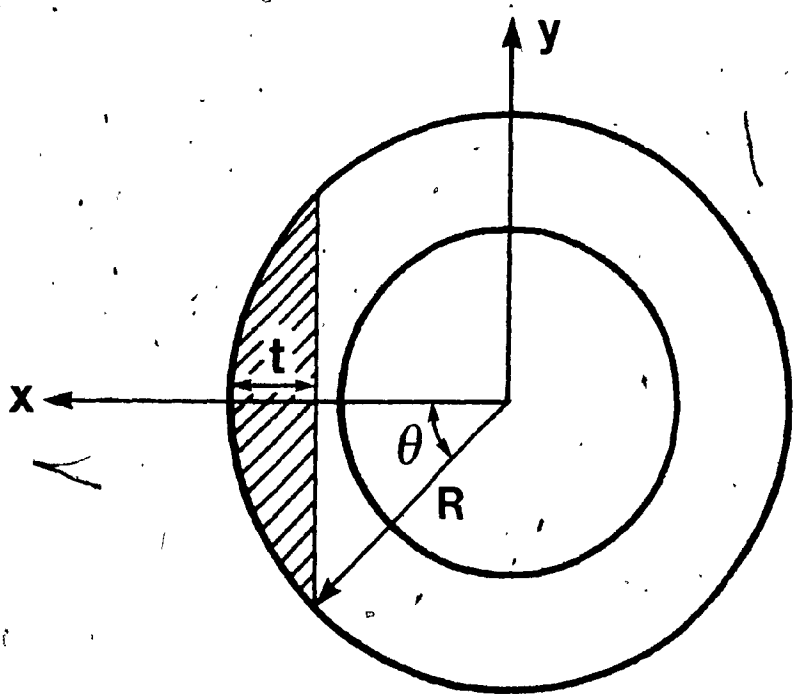

Figure 10. Cross-section of the Torus in the xy Plane

Thus $V = V_P + V_Q$, which is the volume of the torus, may be obtained as a function of the variable t. This volume is the shaded area shown in Figure 10. Values of V for various values of t, converted to percent wear, are given in Table I and are shown in Figure 11.

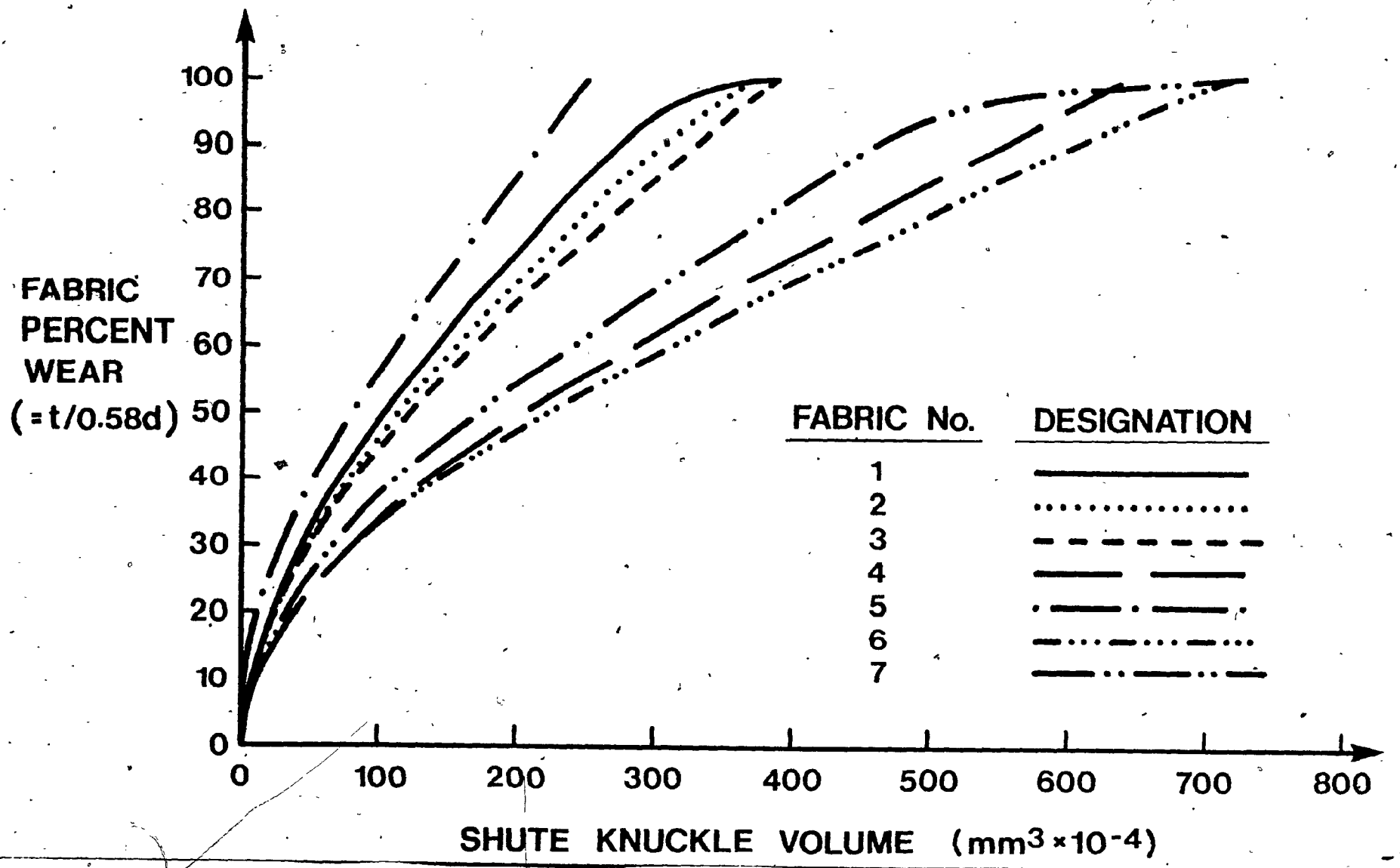

Figure 11. Values of t, converted to Percent Wear, vs. V as determined by the Mathematical Model

CHAPTER 3

EXPERIMENTAL PROCEDURE

3.1. Artificially Induced Wear of Fabric Samples

Wear was induced on samples of various fabric designs on a wear test machine (see Figure 12). The test machine held the samples stationary while a hard blade reciprocated along their bottom surface. The samples, 1½ inches in width, were each tensioned to 15 p.l.i. (pounds per linear inch of width) and with the blade in its foremost position, an angle of wrap of approximately 5° was established.

The blade was composed of a tungsten carbide insert held in a polyethylene block, the complete assembly being mounted in the test machine. The insert was similar to the type used in paper machine foil blades except that its front edge protruded from the polyethylene (as opposed to being level for the paper machine application) in order to induce wear more swiftly.

As many as eight samples could be mounted simultaneously in the test machine, but no more than four fabric designs were studied at the same time: at least two samples of a particular fabric were used for each test so that an average amount of wear could be calculated for that design. Besides careful levelling of the blade, deliberate ordered rotation of the samples among test positions was carried out during a test to prevent any influence that a particular test position might have (e.g. slightly different angle of

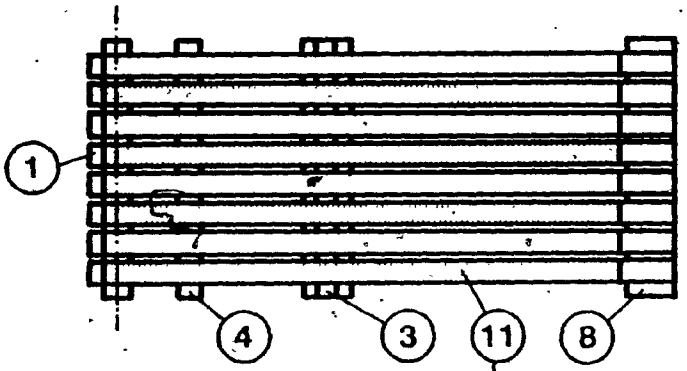

PLAN VIEW

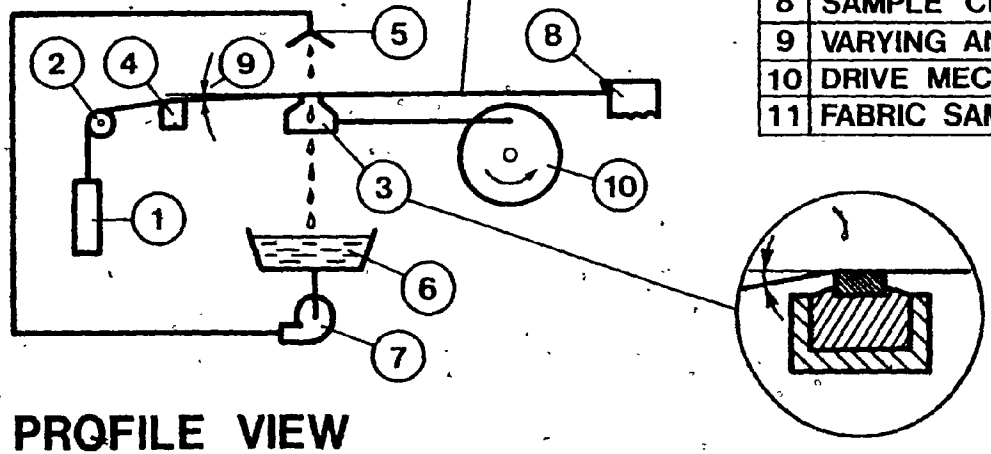

PROFILE VIEW

LEGEND

1	TENSION WEIGHTS
2	PIVOT
3	RECIPROCATING BAR WITH WEARING SURFACE
4	POLYETHYLENE SUPPORT BAR
5	SHOWER NOZZLES
6	WATER RESERVOIR
7	PUMP
8	SAMPLE CLAMP
9	VARYING ANGLE OF WRAP
10	DRIVE MECHANISM
11	FABRIC SAMPLES

Figure 12. The Wear Test Machine

wrap). Each test was usually of one million machine cycles duration with rotation being performed every 250 thousand cycles.

To further reduce discrepancies, the two samples of each fabric sample being tested were run in spaced positions (i.e. position 1 and 5, or 2 and 6) rather than in adjacent positions on the tester. All samples were continually lubricated with water throughout their running time. After each 250,000 cycle run, samples were also repositioned so as to experience the same stroke of the blade over the previously worn area, despite being run in a different position. This ensured that for a given distance from the end of the stroke, each sample would have experienced the same wear action (e.g. the same angle of wrap at each point). It is obvious that due to the varying angle of wrap along the stroke, it would be meaningless to compare one sample at 1" from the end of the stroke with another at 2" from the end of the stroke.

Percent wear was calculated as follows: the thickness of a sample was measured with a micrometer before testing and then after each set of 250,000 cycles. Samples were measured at a point 1/8 inch from the front of the six inch wear strip. This position experienced the maximum angle of wrap on the blade and also the maximum amount of wear. Some other positions along the wear strip were used to check that this measurement was representative of the behaviour of the particular fabric and to ensure that no experimental quirks

had occurred. Readings were always taken along the longitudinal axis in order to avoid the effects of tension variations at the edge.

3.2. Measurement of the Parameters Required for the Experimental Model

The modelling of the shute knuckle as a section of a torus required that an integral be set up and solved to obtain volume as a function of the distance from the outside edge toward the centre. An algebraic expression was obtained giving volume as a function of three variables: the first was the distance mentioned above, the second was the diameter of the strand knuckle and the third was the radius of curvature of the knuckle (Figure 4). Obviously measurements of the second and third variables for each fabric design were required in order to be able to generate curves plotting the volume as a function of distance from the outside edge.

These measurements were obtained by photographing shute strands under a microscope with known magnification. The photomicrographs were then measured physically and these measurements were divided by the magnification to yield the actual dimensions.

3.3. Comparison of Experimental Results with those from the Mathematical Model

Solution of the integral set up for the mathematical model gave an algebraic expression for knuckle volume as a function of the vertical distance through the knuckle. The experimental results gave fabric percent wear for various

numbers of wear cycles on the test machine. In order to be able to compare the results yielded by the mathematical model with the experimental data generated by the test machine, it was necessary to put both sets of information in terms of the same parameters. This was no problem for the vertical coordinate through the knuckle since this variable may easily be converted to percent wear. Zero percent wear occurs at the bottom of the knuckle and 100% wear is defined to be the point 0.58 x the strand diameter from the bottom of the knuckle. A simple linear relationship thus exists between these two variables.

The situation is not quite as simple when one tries to compare test machine cycles with knuckle volume. However since both variables represent resistance to wear of the fabric, the two may be related by means of a scale factor. If the mathematical model was completely accurate, it would be possible for each fabric to multiply each volume produced by the torus integral by the same constant numerical factor to equal the number of cycles required on the test machine to yield that particular percent wear. This method was used and the scale factors were obtained by performing a linear regression analysis between the volumes and number of cycles for each fabric. The scale factor was, of course, the slope of the regression line for the two parameters. These factors are given in Table II. Once they were calculated, the knuckle volumes for each fabric were multiplied by their respective scale factor and the vertical knuckle coordinate,

converted to percent wear, was plotted against the theoretical number of cycles.

CHAPTER 4

EXPERIMENTAL RESULTS

4.1. Comparison of Fabrics with Different Shute Strand Diameters

The first test compared four forming fabrics, (fabric nos 1, 2, 3, 4), all woven with the same four-shed weave pattern, which were virtually identical except for the diameter of their shute strands. Their specifications are given in Table III. Material for the warp strands and for the shute strands is the same for each sample. Warp strand diameters are identical for each type of fabric. Mesh counts differ slightly but not sufficiently to expect them to have a large effect on relative wear resistance of the different fabrics. In any case, these differences were unavoidable since fabric samples identical in every specification except shute strand diameter were unobtainable. Results from the wear experiment on the test machine are given in Table IV.

Comparison of the wear resistance of these fabrics is shown in Figure 13, which plots percent wear against the number of cycles on the test machine. The graph shows the fabric with the smallest shute strand diameter to suffer the most wear over a given time, followed by the two fabrics with the next largest shute diameters. These two fabrics exhibit practically identical wear. The fabric with the largest shute strand diameter suffers the least wear. These results indicate that wear resistance of a forming fabric might well be proportional to the amount of material below the 100% wear

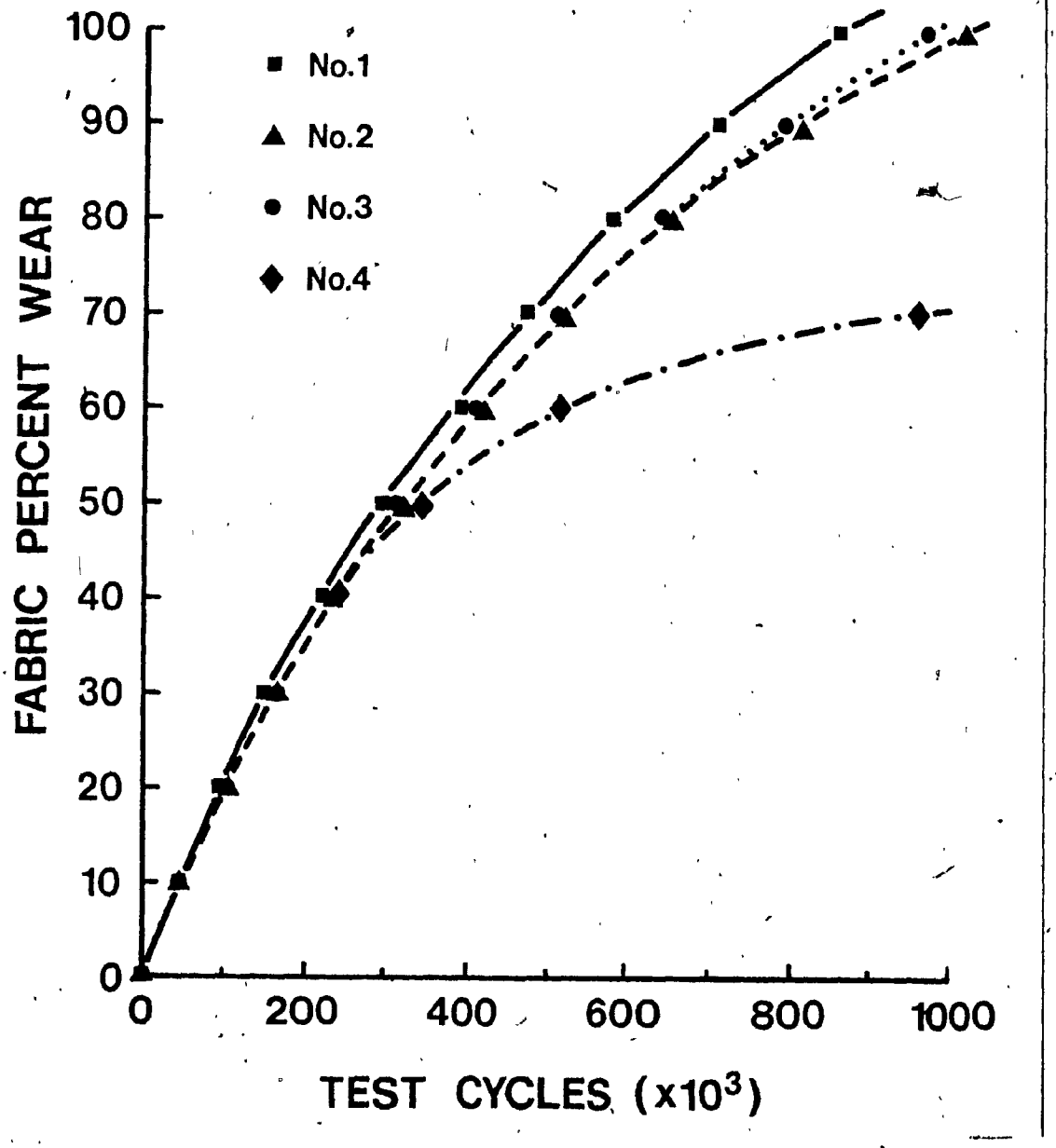

Figure 13. Experimental Results for the Comparison of Four Fabrics with Different Shute Diameters, Fabrics 1,2,3 and 4

plane in the bottom shute knuckles.

4.2. Comparison of a Four-Shed Fabric with a Five-Shed Fabric

This experiment compared two fabrics (fabrics no. 1 and no. 5) which were different in every respect except for their shute strand material. The fact that their warp strand materials are different is unimportant since these strands remain unexposed to wear. Their mesh counts, strand sizes and weave pattern are all quite different (see Table III). Thus this is not a very scientific comparison; however, it is a very relevant comparison from a papermaking viewpoint since the five-shed fabric boasts superior papermaking qualities to the four-shed design and can substitute for it on a papermachine. Its abrasion resistance is suspect though, due to its significantly smaller shute strand diameter. Experimental wear results are listed in Table IV.

Results of comparative testing of these two fabric designs on the testing machine are plotted in Figure 14. The wear resistance of these two fabrics is seen to be virturally identical. However, it is not possible at this stage to determine whether the unexpectedly good abrasion resistance of the five-shed fabric is due to its higher mesh count (65 versus 49 in the cross-machine direction) or to the geometry of its shute strands. Certainly the equal wear resistance of the two fabrics seems due to an equal amount of strand material available for wear up to 100%.

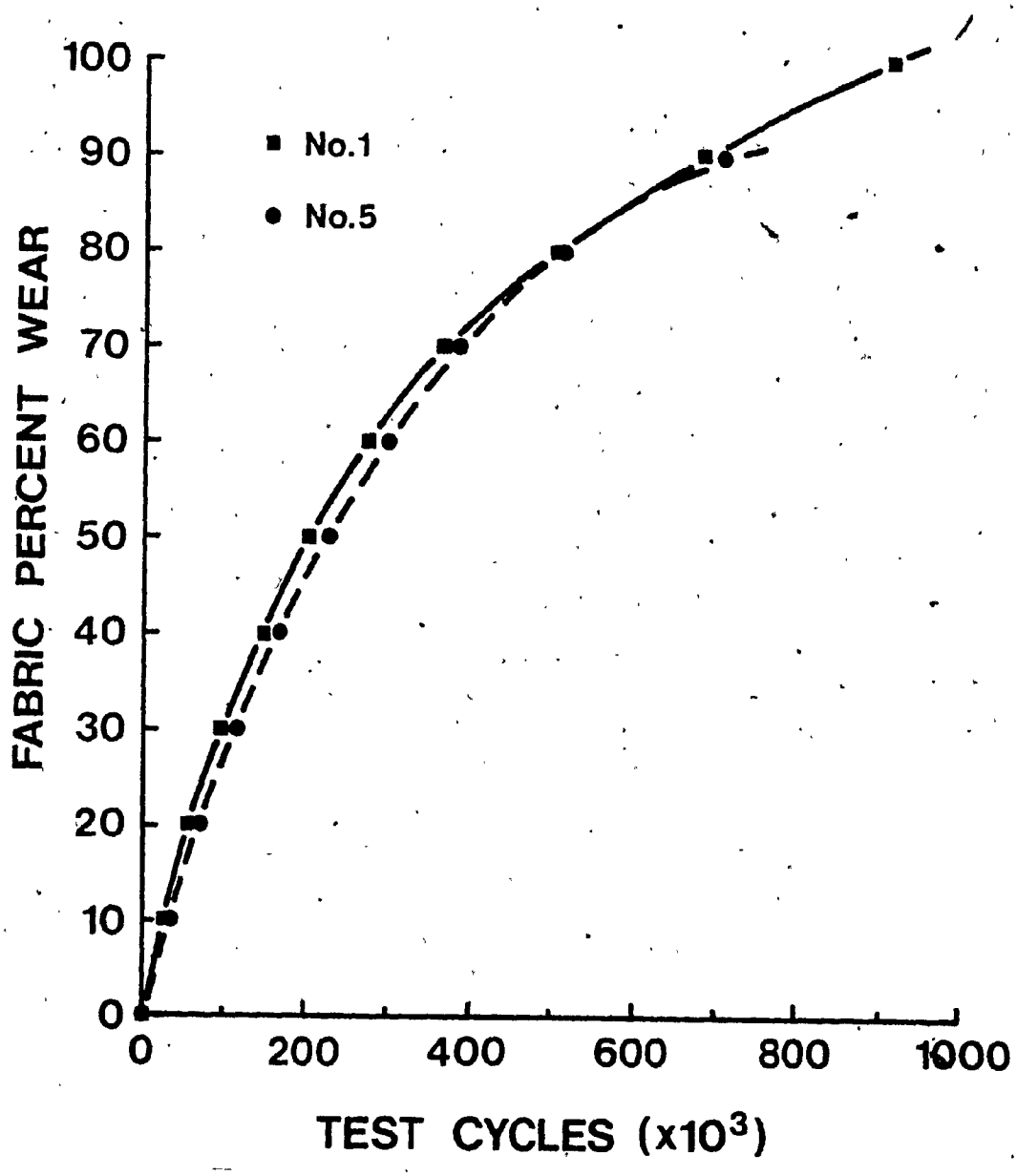

Figure 14. Experimental Results for the Comparison of a Four-shed Fabric with a Five-shed Fabric, Fabrics 1 and 5

4.3. Comparison of Two 56-Mesh Fabrics with Different Warp and Shute Strand Diameters

This comparison dealt with two 56-mesh fabrics (fabric nos. 6 and 7) having virtually identical mesh counts and identical material for both shute strands and also for warp strands. Strand diameters were different for both warp and shute (see Table III for specifications). Test machine cycles vs. percent wear for the two fabrics are given in Table IV.

The results of the wear tests for these two fabrics are plotted in Figure 15. The two designs exhibit equal abrasion resistance. This was originally unexpected due to the larger shute strands in the case of one of the fabrics. Following the results of the previous two tests, it seems possible that the amount of material in a shute knuckle below the 100% wear plane is equal in both fabrics.

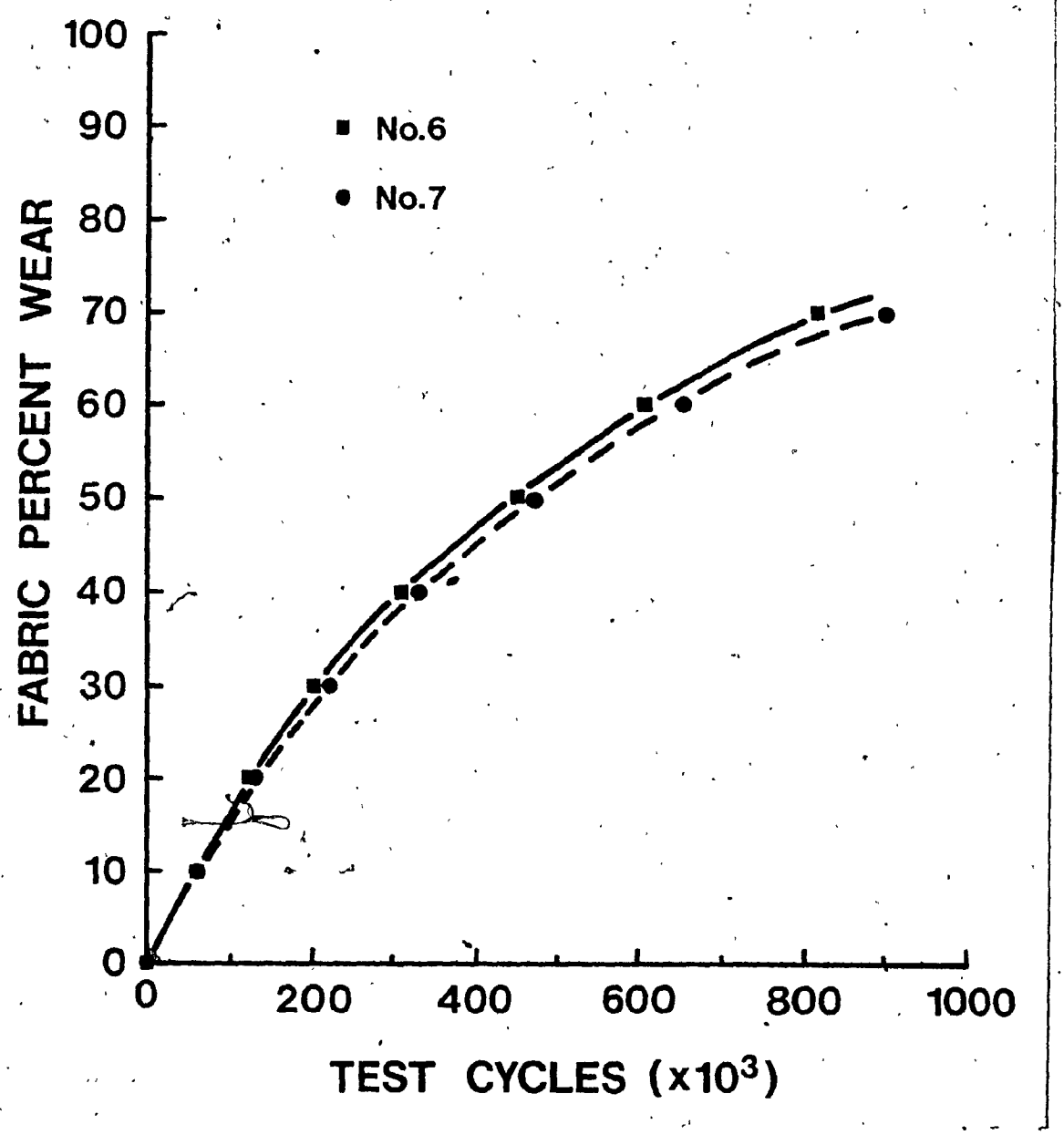

Figure 15. Experimental Results for the Comparison of Two 56-Mesh Four-shed Fabrics, Fabrics 6 and 7

CHAPTER 5

EVALUATION OF THE EXPERIMENTAL MODEL

After determination of the scale factor for each fabric, the knuckle volume data generated by the mathematical model and listed in Table I was multiplied by the appropriate scale factors to yield the number of cycles predicted to reach the various percent wear values. The number of cycles for each fabric are listed in Table V. This data was then plotted as percent wear versus predicted cycles on the same graph as the experimental percent wear cycles results (from Table IV) for each fabric. This permitted an evaluation of how well the mathematical model predicted the wear behaviour or various forming fabrics.

The actual and predicted numbers of cycles required to reach 0 to 100% wear for all the fabrics studied are given in Figures 16 - 22. Curves are drawn for the wear predicted by the mathematical model. The experimental data on each graph is indicated with circles. For all fabrics, the experimental points lie very close to the predicted wear curves, especially at relatively high numbers of cycles. The error is greater at the beginning of the wear curve because the shute knuckles have a relatively small contact area early in the life of the fabric. As previously mentioned, they start out with virtually point contact, so that a more rough, gouging type of abrasion will take place at first. But as the knuckle area increases in size, the wear rate decreases and the wearing action itself becomes smoother; it more closely

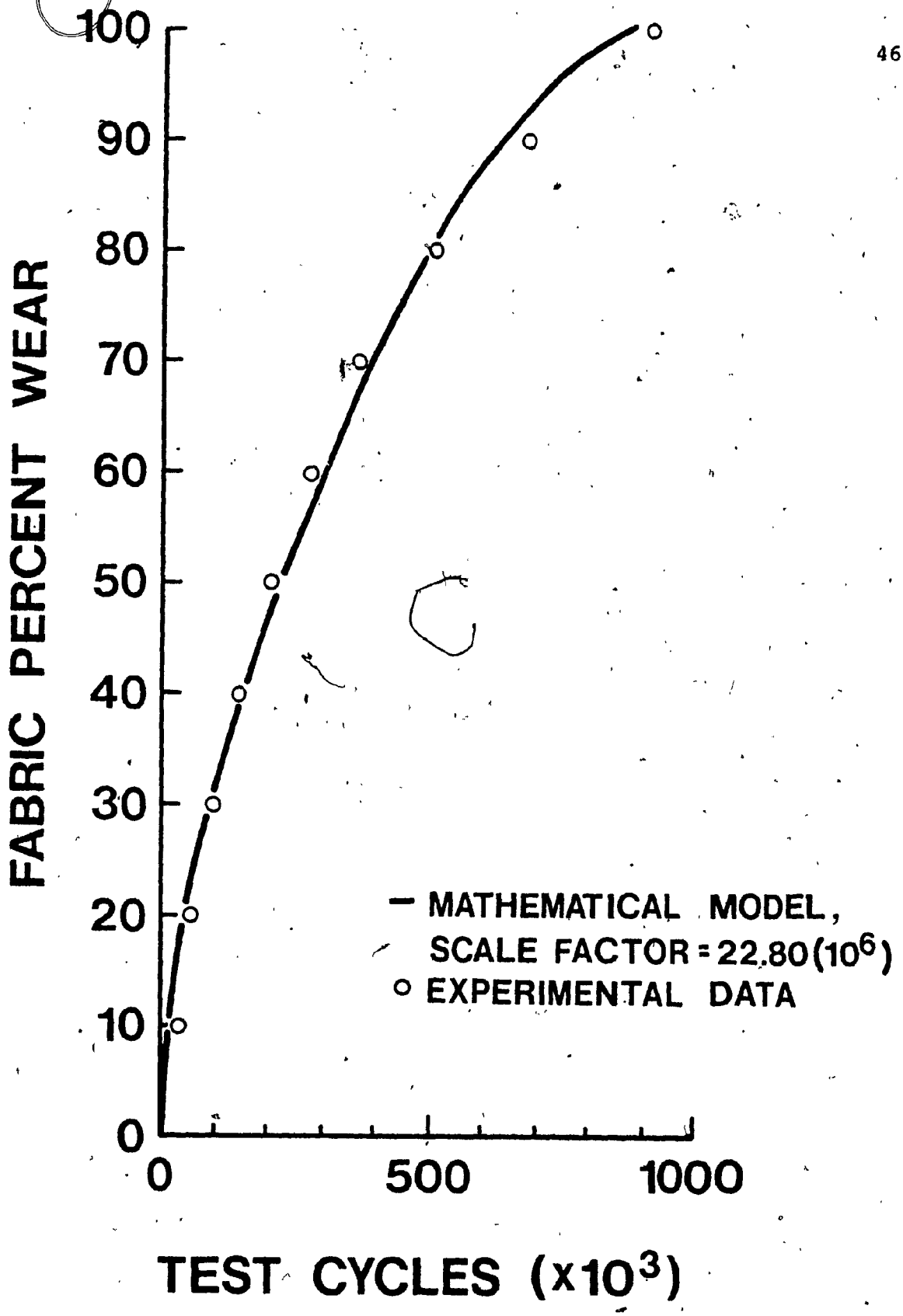

Figure 16. Fabric Percent Wear vs. Test Cycles for Fabric No. 1

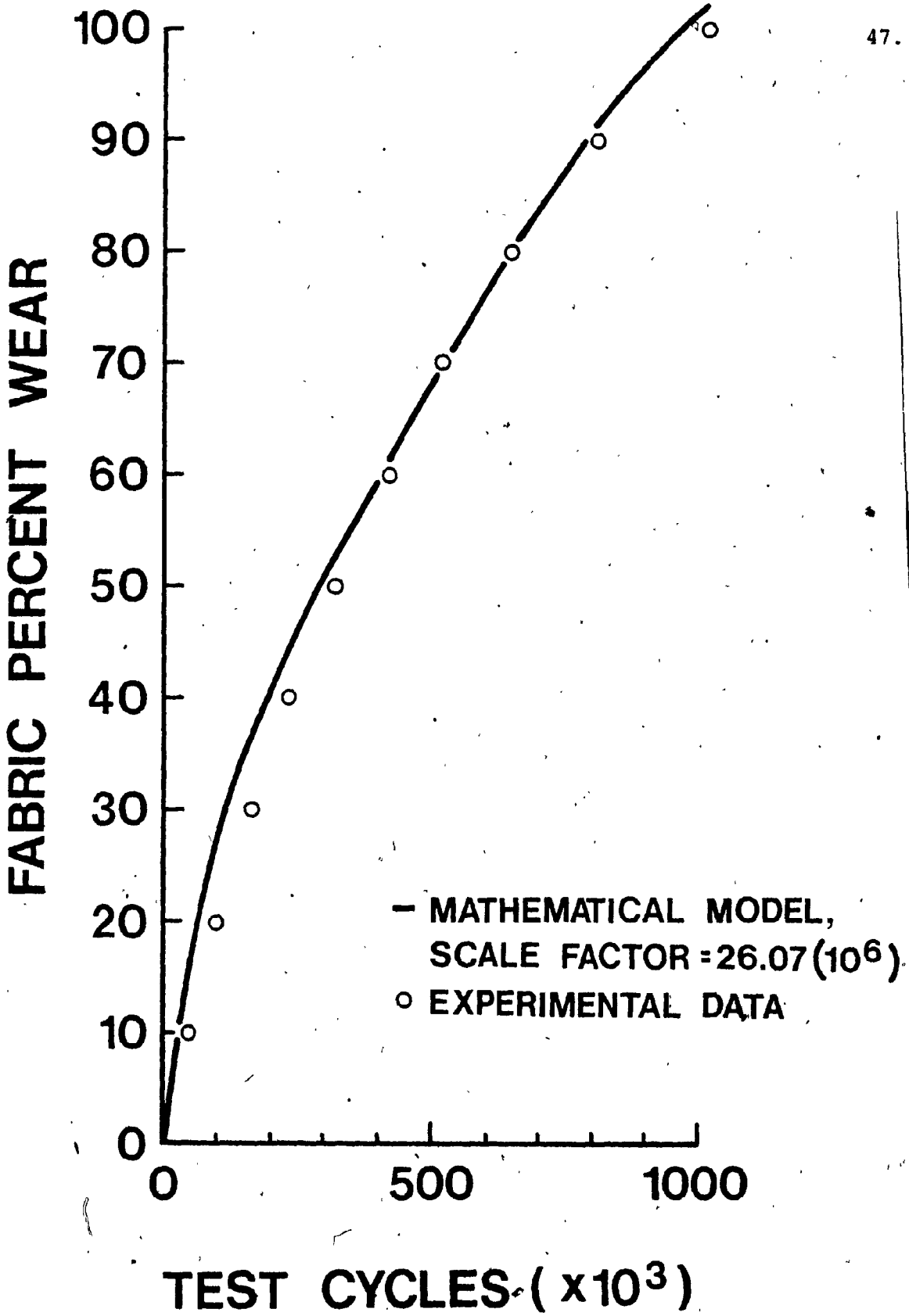

Figure 17. Fabric Percent Wear vs. Test Cycles for Fabric No. 2

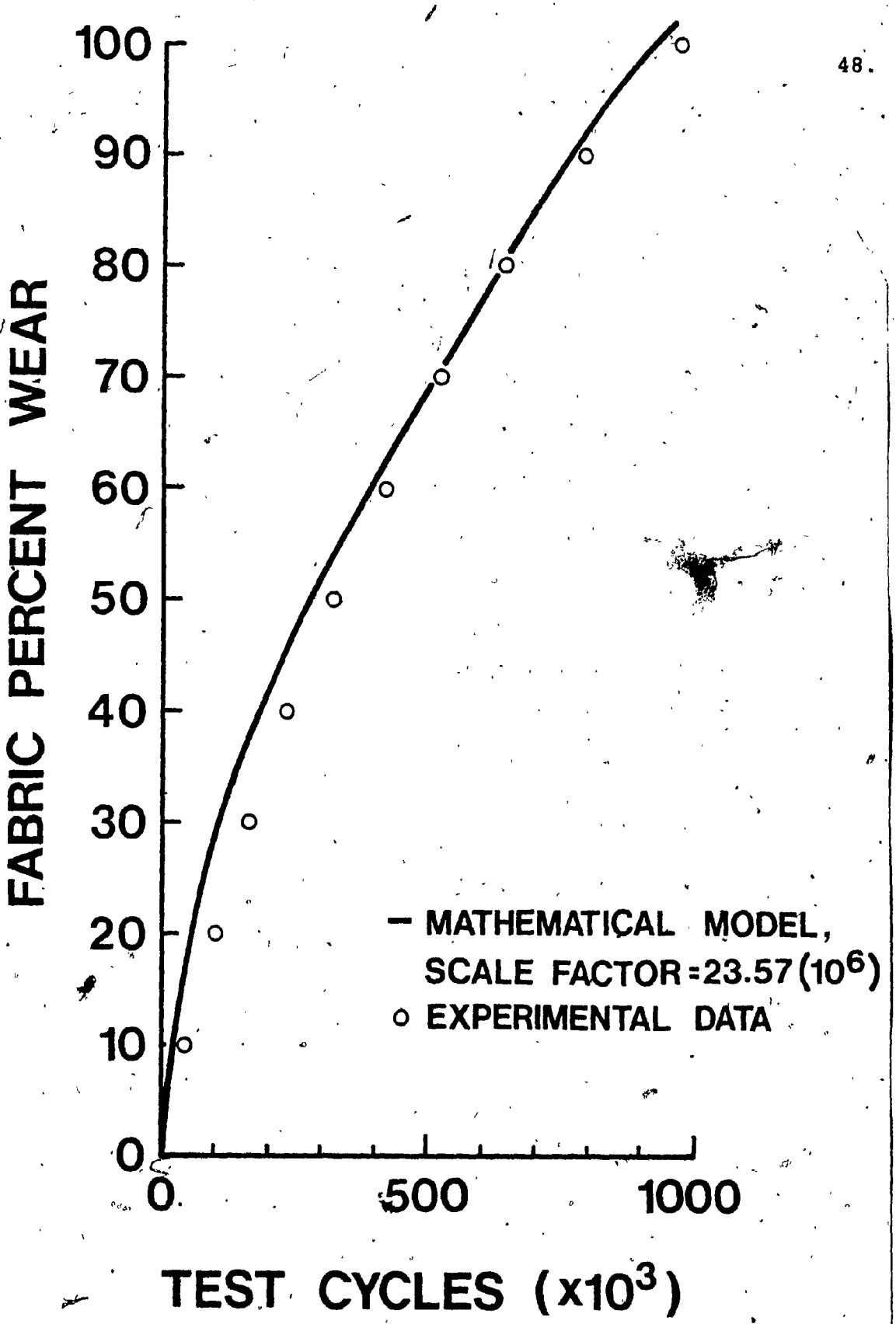

Figure 18. Fabric Percent Wear vs. Test Cycles for Fabric No. 3

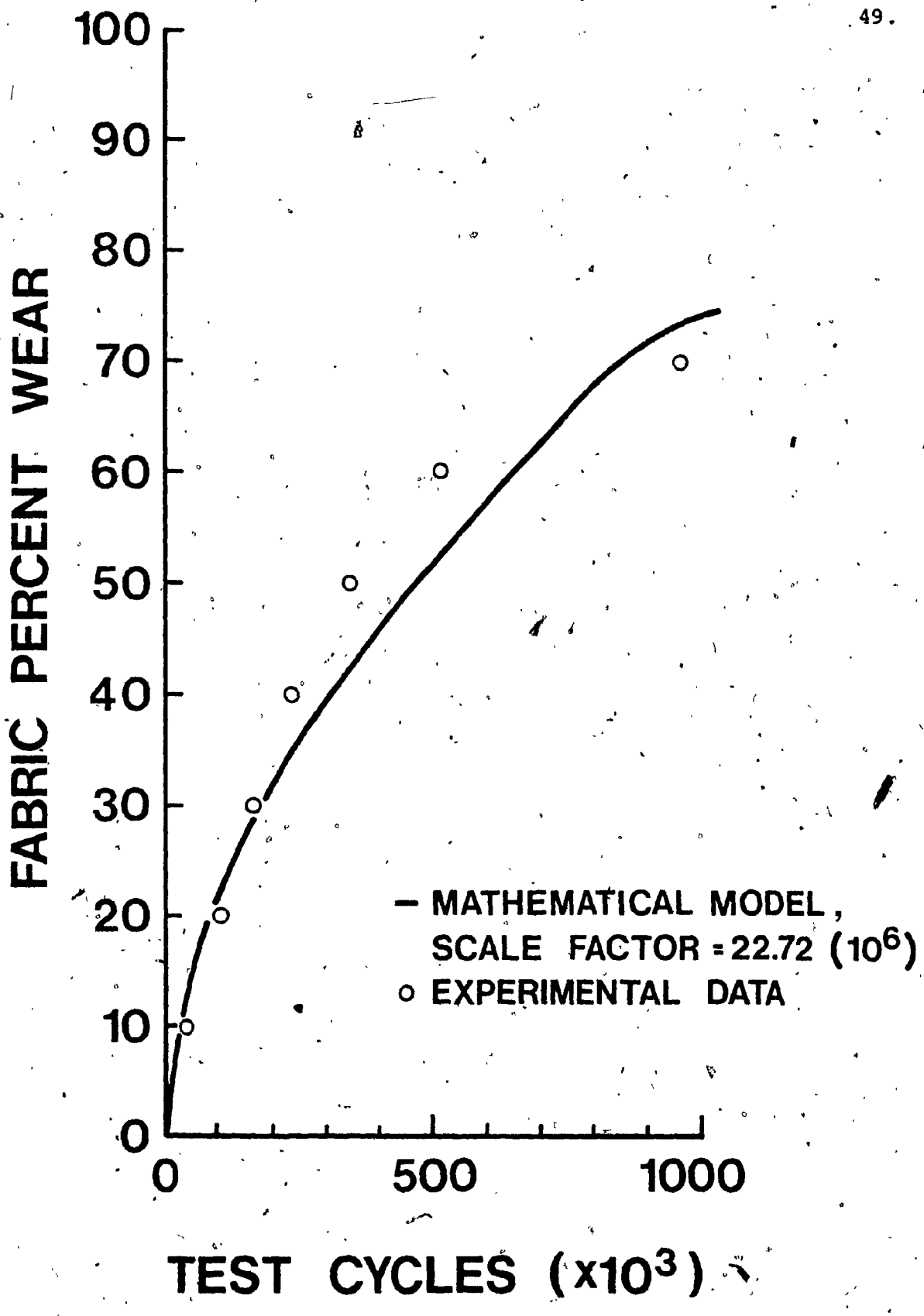

Figure 19. Fabric Percent Wear vs. Test Cycles for Fabric No. 4

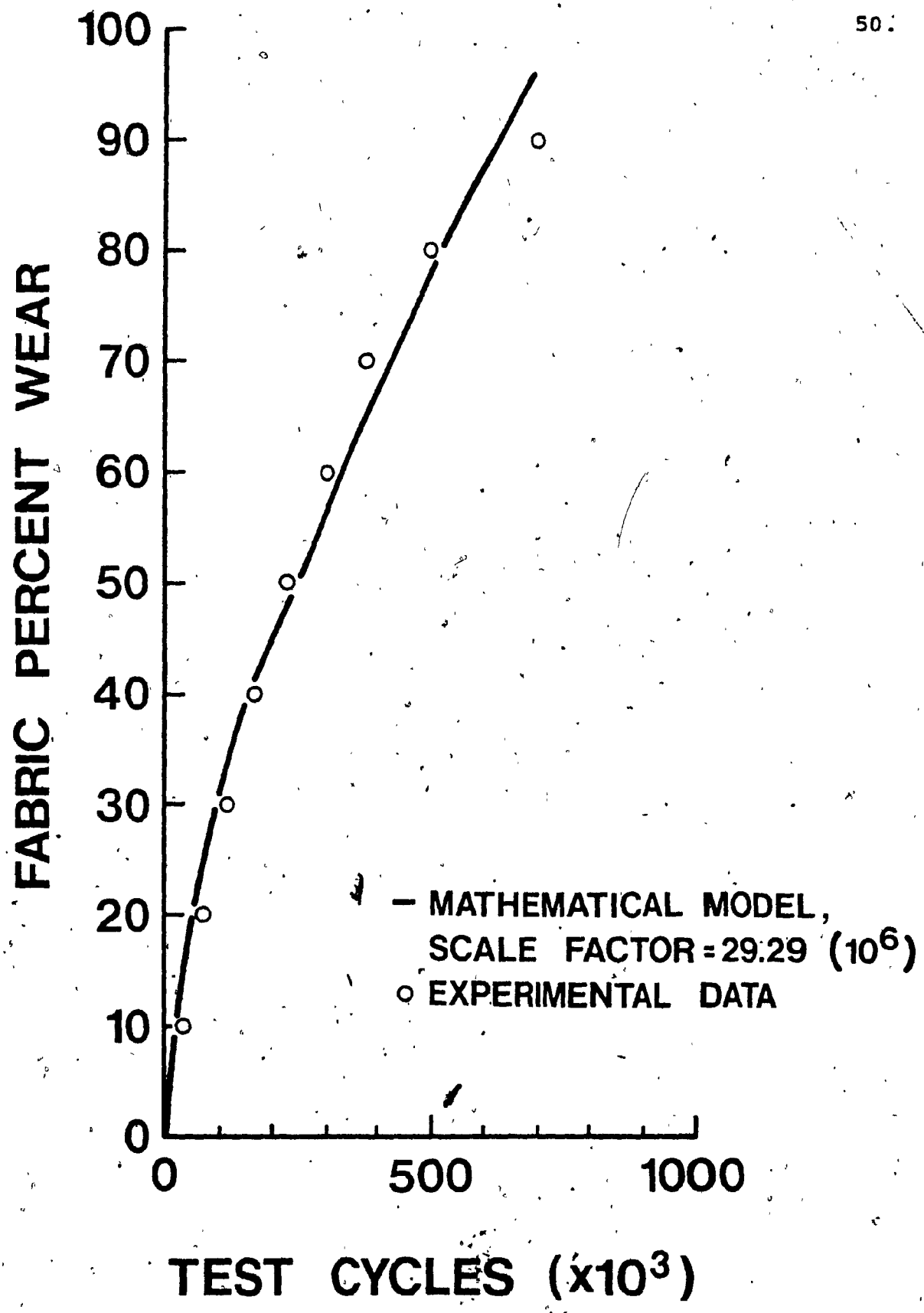

Figure 20. Fabric Percent Wear vs. Test Cycles for Fabric No. 5

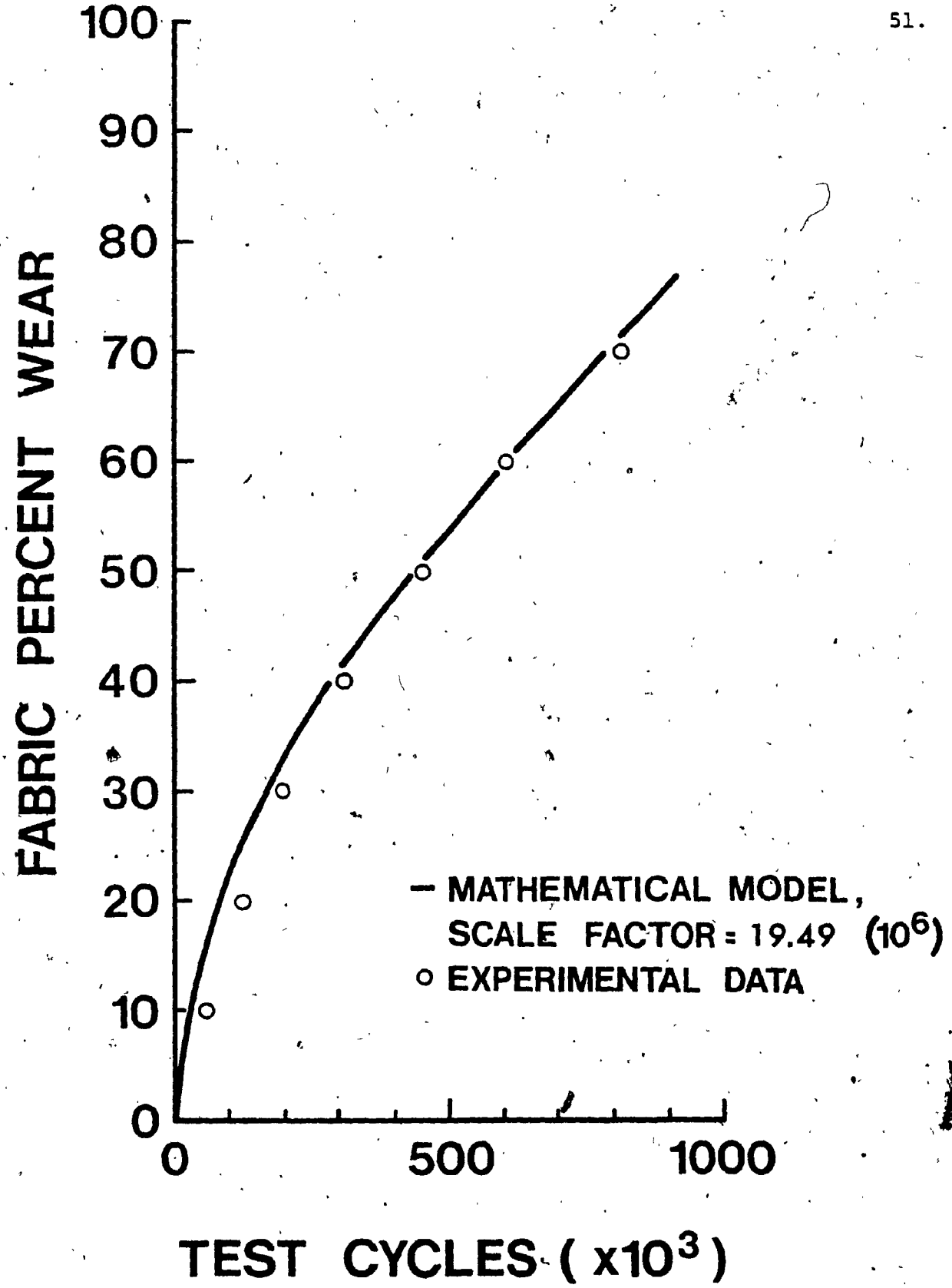

Figure 21. Fabric Percent Wear vs. Test Cycles for Fabric No. 6

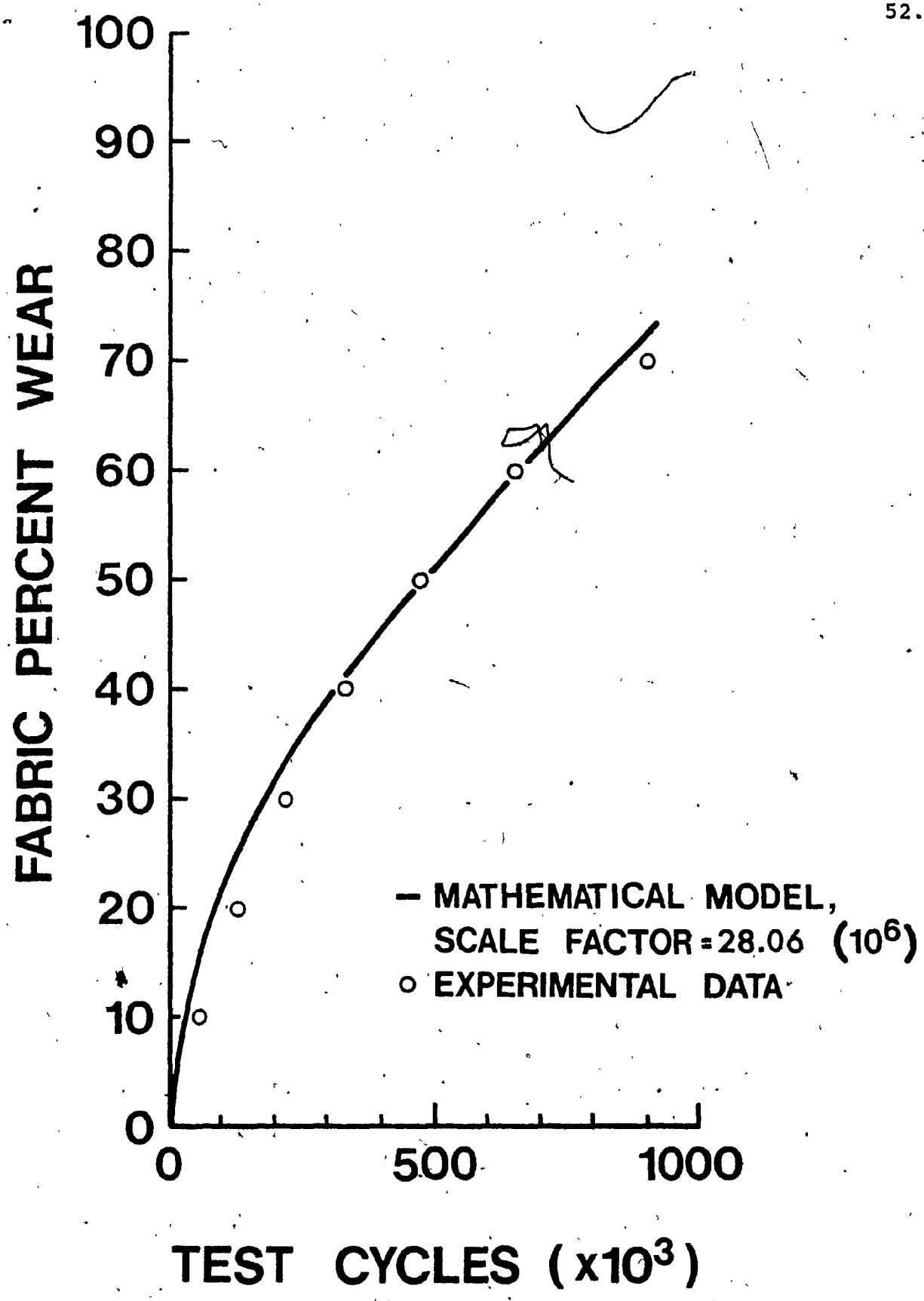

Figure 22. Fabric Percent Wear vs. Test Cycles for Fabric No. 7

resembles the cutting of slices off the bottom of the knuckles.

It should be kept in mind that the test machine was intended to simulate a papermachine from an abrasion viewpoint. It was not meant to be a sophisticated piece of equipment which very carefully and slowly produced even, smooth wear on fabric samples. A variation of as much as 5% wear across the width of the sample was known to occur. This variation alone could account for the differences between experimental and predicted results. Other errors were of course present in the measurement of worn sample caliper. However, despite these experimental sources of error, the torus appears to be an excellent model of the bottom shute knuckle of a forming fabric. Use of the model allows the fabric manufacturer to know before installation on a papermachine how a particular fabric will resist abrasion compared to its predecessors.

The appendix gives a derivation of a non-dimensional expression for the mathematical model which may be used to predict how different fabric designs compare from a wear viewpoint. The non-dimensionalized volume is plotted in Figure 23 against the non-dimensionalized percent wear for various values of the diameter ratio R/r.

CHAPTER 6

DISCUSSION, CONCLUDING REMARKS AND RECOMMENDATIONS

The results presented here yield several conclusions concerning the wear of forming fabrics. Due to the curvature of the cross-machine direction knuckles and the fact that they lie lower in the fabric than the machine direction strands, the wear rate of the forming fabric gradually decreases as wear progresses. As each individual bottom shute knuckle wears, its bottom surface increases in area from virtually initial point contact with stationary paper machine components. As the bottom area of the knuckle increases, a progressively smaller thickness of material will be removed during each rotation of the fabric around the paper machine or during each stroke on the test machine. In other words, the shape of the wear curves from commercial paper machines (4) or from this study indicate that approximately the same volume of material rather than the same thickness is removed during each rotation on the machine or during each stroke on the test machine. The reason for this seems most likely to be the reduced loading on the knuckles as their surface area increases. Wear theory states that severity of abrasion is dependent on the normal force between the two surfaces (11). Thus the virtually constant weight of the stock will be spread over a larger area resulting in progressively less interlocking at the microscopic level of the fabric surface with the various surfaces on the paper machine.

The fact that the shute knuckles form the bottom

surface of a fabric without help from the warp strands means that even after substantial wear has occurred, only a small percentage of the fabric's complete area will contact the paper machine components. Unfortunately, designing a fabric so as to have both warp and shute strands available for wear can have dangerous consequentes. Wear on the warp strands could result in a loss of elastic modulus and the stretching of the fabric off the paper machine. (Paper machines have a relatively small range of possible fabric lengths).

Since forming fabrics must first be designed for their papermaking qualities and secondly for abrasion resistance, several constraints are imposed on any possible modifications to improve fabric life. But successful modifications do exist. Increasing shute strand size for the four-shed fabrics made more strand material available for wear and in one case significantly increased fabric life. However, for the 56-mesh four-shed fabrics, increasing both warp and shute strand diameters produced increased curvature of the shute strand knuckles. The result of this was no significant change in the amount of material available for wear resistance. As long as papermaking qualities are not affected, increasing shute strand diameter (and not warp strand diameter) will increase fabric life.

The use of different weave pattern, the five-shed instead of the four-shed, proved to be extremely effective in providing resistance to abrasion. The five-shed fabric

was seen to wear at the same rate as a four-shed fabric with a 14% larger shute strand. The reason for this was seen to be the smaller curvature of the bottom shute knuckles in the five-shed design.

The mathematical model presented predicts the relative abrasion resistances of various forming fabrics. The bottom shute knuckles of four and five-shed fabrics are well modelled by a section of a torus. The theoretical curves developed closely approximate those obtained with the experimental wear tester. The differences between the two are readily explained by experimental error. Variations in worn caliper across the experimental samples could singlehandedly be responsible for these differences. Errors due to the variation of both new sample thickness and strand diameters were minimized by measuring a large number of samples.

In conclusion, the problem of fabric wear is unlikely to disappear in the near future since it is not quite the priority it was in the days of bronze wires. Other areas in the papermaking process present far more potential for reducing costs. However, the use of a mathematical model can assist the choice of forming fabric for a particular application by maximizing the life potential of the fabric.

RECOMMENDATIONS

1) Experimental work should be performed on forming fabrics with identical specifications except for shute material. In this way the mathematical model could be modified to include a factor dependent on the type of shute strand material.

2) Information should be gathered from commercial paper-machines to relate the life of a particular design of fabric to machine speed and production of paper. The mathematical model could then be used to help design a fabric which would minimize fabric cost per ton of paper under papermaking and operating constraints.

REFERENCES

1. Pye, I.T., Wear of Fourdrinier Wire Bearing Materials, Pulp and Paper Mag. Canada 59(3):124-139 (1958).

2. Bratt, R.L. and McNamara, A.J., Some Mechanical Aspects of Wire Wear and A Method to Study the Wear, Pulp and Paper Mag. Canada 71(3):44 (1970).

3. MacDonald, C.E., et al., Study of Newsprint Machine Wire Life, Pulp and Paper Mag. Canada 60(C):185 (1959).

4. Pitt,R., Wear of Forming Fabrics, Tappi 62,1 (1979).

5. Condon, E.M., How Drag Load Affects Slip and Creep, Pulp and Paper 49(12):120 (1975).

6. Lawson, J.J.A. and Lambert, J.E., Newsprint Machine Wire Life and Silicon Carbide Flatbox Covers, Pulp and Paper Mag. Canada, 63(11):T-544 (1962).

7. Fuchs, K.D., Wire, Cover and Filler Materials - Their Significance and Influence on the Wear Meachanism, Trans. Wockenblatt Fur Papier Fabrikation, 103(10):348 (1975).

8. Johnson, D.B., A Review of Fabric Operating Characteristics, Tappi 59(10):57 (1976).

9. Turner, D.H., Synthetic Forming Fabrics: their History, Present and Future Status, Pulp and Paper 50(12):88 (1976).

10. Friese, J., The Improvement of Paper Machine Wire Life, Pulp and Paper Mag. Canada 61(10):T-474 (1960).

11. Bowden, F.P. and Taber, D., Friction and Lubrication of Solids, O.U.P., 1954.

Table I. Volumes ($mm^3 \times 10^{-4}$) of the Shute Knuckle for the Various Fabrics studied as determined by the Mathematical Model

PCW	FABRIC NO.						
	1	2	3	4	5	6	7
0	0	0	0	0	0	0	0
10	5	5	5	9	4	10	8
20	18	20	21	36	14	39	30
30	38	43	46	78	31	85	65
40	66	73	79	134	53	146	111
50	99	111	119	202	80	220	167
60	137	153	165	280	110	304	232
70	178	200	215	365	143	397	302
80	222	249	267	455	178	495	376
90	266	299	321	547	214	594	451
100	382	369	389	637	-	712	699

Table II. Scale Factors to convert Volumes obtained from the Mathematical Model to Cycles (as determined by regression analysis)
Volume values must be multiplied by this figure to be expressed as cycles for the mathematical model

FABRIC	SCALE FACTOR (Million Cycles/mm^3)
1	22.80
2	26.07
3	23.57
4	22.72
5	29.29
6	19.49
7	28.06

Table III. Fabric Designation Numbers and Specifications

FABRIC DESIGNATION NUMBER	WEAVE PATTERN	MESH	WARP STRAND DIAMETER (mm)	SHUTE STRAND DIAMETER (mm)
1	4-SHED	73x49	0.210	0.224
2	4-SHED	72x50	0.210	0.238
3	4-SHED	72x48	0.210	0.245
4	4-SHED	70x45	0.210	0.300
5	5-SHED	85x65	0.170	0.196
6	4-SHED	57x40	0.280	0.300
7	4-SHED	56x40	0.250	0.270

Table IV. Experimental Results, Test Cycles (x 1000) to reach Various Percent Wear Values

PCW	FABRIC NO.						
	1	2	3	4	5	6	7
0	0	0	0	0	0	0	0
10	28	45	45	45	33	60	60
20	58	100	100	100	70	125	130
30	95	165	165	165	113	200	220
40	148	235	235	235	165	310	330
50	203	320	320	340	228	450	470
60	273	420	420	510	298	605	650
70	365	520	520	960	380	815	900
80	505	650	640	-	500	-	-
90	680	810	790	-	705	-	-
100	915	1020	970	-	-	-	-

Table V. Data generated by the Mathematical Model multiplied by Scale Factors to give Predicted Test Cycles (x 1000) for Various Percent Wear Values

PCW	FABRIC NO.						
	1	2	3	4	5	6	7
0	0	0	0	0	0	0	0
10	10	13	13	21	11	20	21
20	40	51	50	81	41	76	83
30	87	111	108	177	90	165	181
40	150	191	186	305	155	284	312
50	225	288	280	459	233	428	470
60	312	399	388	636	323	593	650
70	406	521	506	830	420	774	847
80	506	648	630	1035	522	964	1054
90	607	778	756	1243	626	1157	1264
100	870	962	917	1448	-	1387	1961

APPENDIX

It is possible to non-dimensionalize the equation for the volume of the shute knuckle in order to generalize the mathematical model for any fabric whose parameters r and R are given. Now

$$V = V_P + V_Q \tag{1}$$

and $$V_P = \frac{4}{3}\,\delta\theta\,\left(R^3 - \frac{\beta^3 (R-r)^3}{\gamma}\right) \tag{2}$$

Since $$\beta = \frac{R-t}{R-r} \tag{3}$$

Substituting equation (3):

$$V_P = \frac{4}{3}\,\delta\theta\,\left[\left(\frac{R}{r}\right)^3 - \frac{1}{\gamma}\left(\frac{R-t}{r}\right)^3\right] \tag{4}$$

or $$\frac{3V_P}{4r^3} = \delta\theta\,\left[\left(\frac{R}{r}\right)^3 - \frac{1}{\gamma}\left(\frac{R-t}{r}\right)^3\right] \tag{5}$$

Letting $\frac{t}{r} = J$, $\frac{R}{r} = K$ and $\frac{R-t}{r} = L$ (6,7,8)

and substituting, we obtain

$$\frac{3V_P}{4r^3} = \delta\theta\,\left(K^3 - \frac{L^3}{\gamma}\right) \tag{9}$$

Since $$\theta = \cos^{-1}\frac{R-t}{r} \tag{10}$$

and since

$$\delta = \sqrt{1 - \frac{\beta^2}{\alpha^2 - 1 + 2\beta}} \qquad \gamma = \frac{\beta}{\sqrt{\alpha^2 - 1 + 2\beta}} \tag{11,12}$$

Substituting in equation (9)

$$\frac{3V_P}{4r^3} = \sqrt{1 - \frac{\beta^2}{\alpha^2 - 1 + 2\beta}}\;\cos^{-1}\left(\frac{R-t}{r}\right)\left[K^3 - L^3\sqrt{\frac{\alpha^2 - 1 + 2\beta}{\beta}}\right] \tag{13}$$

Substituting equations (6,7,8) and simplifying

$$\frac{3V_P}{4r^3} = \sqrt{1 - \frac{\alpha^2L^2}{\alpha^2-1+2\beta}}\ (\cos^{-1}\frac{L}{K})(K^3 - \frac{L^2}{\alpha}\sqrt{\alpha^2-1+2\alpha L}) \qquad (14)$$

Now $$V_Q = \frac{4}{3}\theta(R-t_o)^3\{\frac{3\alpha^4}{8} - \frac{3\delta^4}{8}\} + \frac{4}{3}\theta\beta^3(R-r)^3\{\frac{\gamma}{\delta} - \sqrt{\frac{1-\alpha^2}{\alpha^2}}\} \qquad (15)$$

and $$t_o = \frac{Rr}{R-r} \qquad (16)$$

Substituting equations (6,7,8,10,11,12,16) and simplifying, one obtains

$$\frac{3V_Q}{4r^3} = \{\cos^{-1}\frac{L}{K}\}\{\frac{3}{8}K^3(1-\alpha)\{\alpha^4 - (1 - \frac{\alpha^2L^2}{\alpha^2-1+2\alpha L})^2\} + L^3(\frac{\alpha L}{\sqrt{\alpha^2-1+2\alpha L-\alpha^2L^2}} - \sqrt{\frac{1-\alpha^2}{\alpha^2}})\} \qquad (17)$$

Setting $$V_N = \frac{3V_P}{4r^3} + \frac{3V_Q}{4r^3} \qquad (18)$$

we now have a dimensionless expression for the shute knuckle volume in terms of dimensionless parameters. It is now possible to plot J(=t/r), which is analagous to percent wear, vs. V_N for the different fabrics. This is given in Figure 23.

The parameter K(=R/r) is different for each fabric. Plotting J vs. V_N for the various fabrics yields a family of curves for which the value of K increases from left to right. For each comparison undertaken in this study, the most wear resistant fabric lies to the left of the one or ones against which it was tested. We may therefore conclude that to increase fabric abrasion resistance for a given design

of fabric, the parameter K should be decreased as much as possible subject of course to the constraints imposed by papermaking.

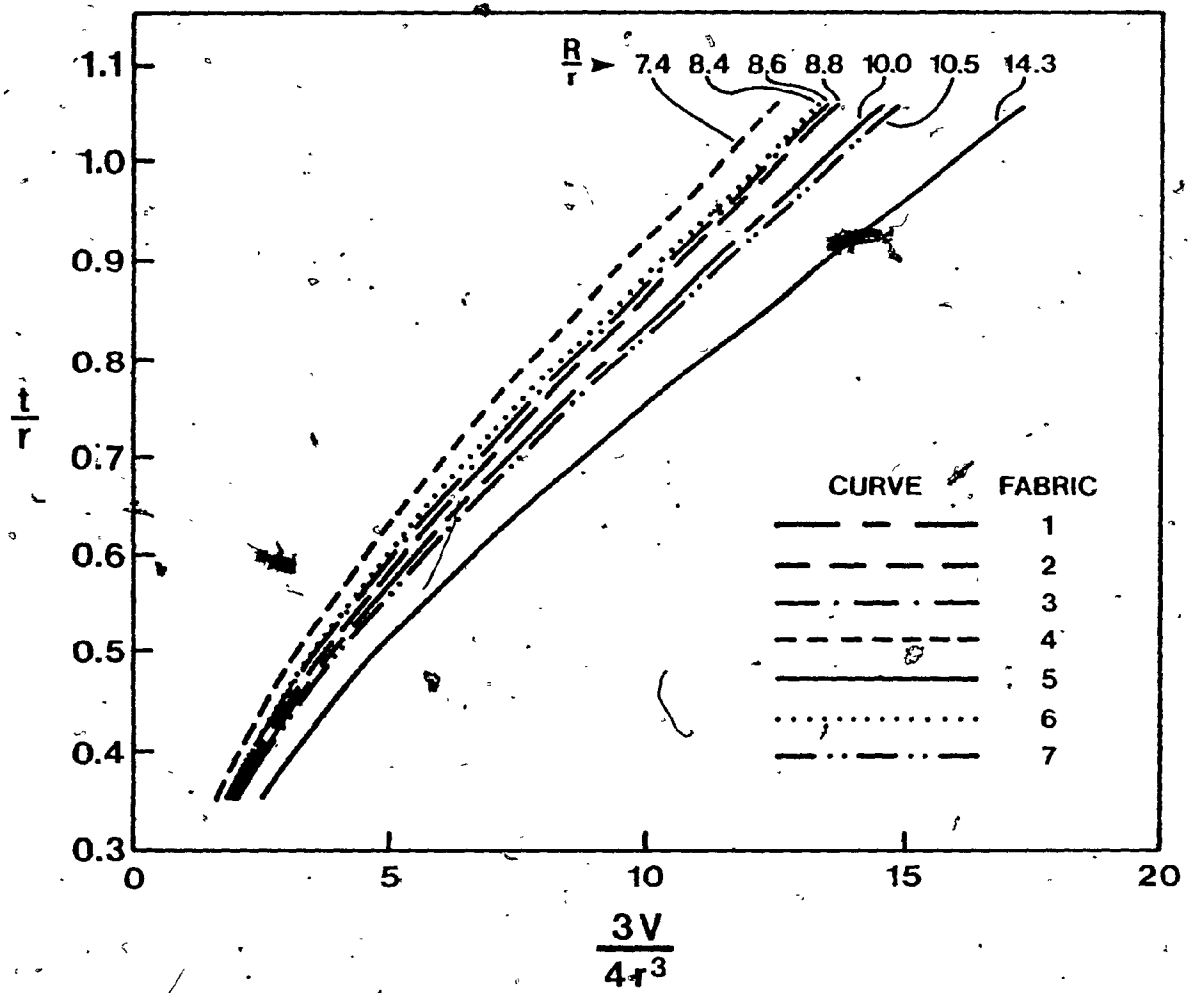

Figure 23. Dimensionless vertical shute knuckle coordinate vs. dimensionless shute knuckle volume for the various fabrics studied.